ELSEVIER

Journal of Organometallic Chemistry 626 (2001) 243–259

Journal of Organometallic Chemistry

www.elsevier.nl/locate/jorganchem

1,4-Diaza-1,3-diene (DAD) complexes of early transition elements. Syntheses, structures and molecular dynamics of mono- and bis(η^5-cyclopentadienyl)titanium-, zirconium- and hafnium(DAD) complexes. Crystal- and molecular structures of $CpTi(DAD)CH_2Ph$, $[CpTi(DAD)]_2O$, $CpZr[(DAD)(N^{\frown}O)]$ and $Cp_2Hf(DAD)$

Joachim Scholz [a,*], Ghasan A. Hadi [b], Karl-Heinz Thiele [b], Helmar Görls [c], Roman Weimann [d], Herbert Schumann [d], Joachim Sieler [e]

[a] *Universität Koblenz-Landau, Institut für Chemie, Rheinau 1, D-56075 Koblenz, Germany*
[b] *Martin-Luther-Universität Halle-Wittenberg, Institut für Anorganische Chemie, Geusaer Straße, D-06217 Merseburg, Germany*
[c] *Friedrich-Schiller-Universität Jena, Institut für Anorganische und Analytische Chemie, Lessingstraße 8, D-07743 Jena, Germany*
[d] *Technische Universität Berlin, Institut für Anorganische und Analytische Chemie, Straße des 17. Juni 135, D-10623 Berlin, Germany*
[e] *Universität Leipzig, Institut für Anorganische Chemie, Linnéstraße 3, D-04103 Leipzig, Germany*

Received 12 October 2000; received in revised form 9 January 2001; accepted 30 January 2001

Abstract

Treatment of $CpTiCl_3$ and $CpZrCl_3(THF)_2$ with one equivalent magnesium in the presence of 1,4-diaza-1,3-dienes ($R^1N{=}CR^2CR^2{=}NR^1$ (R^1,R^2-DAD; $R^1 = C_6H_4$-2-Me, C_6H_4-4-Me, C_6H_4-4-OMe, $R^2 = H$, Me, Ph) yields the monomeric titanium complexes CpTi(R^1,R^2-DAD)Cl (**2**, $R^1 = C_6H_4$-4-OMe, $R^2 = H$; **3**, $R^1 = C_6H_4$-2-Me, $R^2 = Me$; **4**, $R^1 = C_6H_4$-4-OMe, $R^2 = Me$; **5**, $R^1 = C_6H_4$-4-Me, $R^2 = Ph$), and the chloro bridged dimeric zirconium complexes $[CpZr(R^1,R^2\text{-DAD})Cl]_2$ (**6**, $R^1 = C_6H_4$-4-OMe, $R^2 = H$; **7**, $R^1 = C_6H_4$-4-OMe, $R^2 = Me$; **8**, $R^1 = C_6H_4$-4-Me, $R^2 = Ph$). Both the half-sandwich complexes of DAD ligands bearing alkyl (**3**, **4** and **7**) and aryl (**5**, **8**) substituents at the inner carbon atoms and the complexes without substituents at this DAD positions (**2**, **6**) prefer the σ^2,π-coordination geometry with a *supine* conformation of the heterodiene. Alkylation of the new half-sandwich DAD complexes with one equivalent of $PhCH_2MgCl$ or one equivalent of MeMgI affords the benzyl and methyl derivatives $CpM(R^1,R^2\text{-DAD})CH_2Ph$ (**9**, M = Ti, $R^1 = C_6H_4$-4-OMe, $R^2 = Me$; **10**, M = Zr, $R^1 = C_6H_4$-4-OMe, $R^2 = Me$) and $CpZr(R^1,R^2\text{-DAD})Me$ (**11**, $R^1 = C_6H_4$-4-Me, $R^2 = Ph$). An X-ray study of the benzyl derivative **9** reveals that the alkylation does not change appreciably the DAD bonding parameters in comparison with the starting chloride complex **4**. The monomeric half-sandwich zirconium complex $CpZr(R^1,R^2\text{-DAD})(N^{\frown}O)$ (**12**, $R^1 = C_6H_4$-4-OMe, $R^2 = H$) which has been prepared by reaction of **6** with the chelating acetylacetoneiminate compound $Na[(C_6H_4\text{-}4\text{-}Me)N{=}C(Me)\text{-}CH{=}C(Me)O]$ ($Na[N^{\frown}O]$) as well as the oxygen bridged complex $[CpTi(R^1,R^2\text{-DAD})]_2O$ (**13**, $R^1 = C_6H_4$-2-Me, $R^2 = Me$) which has been formed by hydrolysis of **3** also keep the *supine* conformation of the heterodiene ligand with respect to the Cp group. Temperature dependent NMR spectra of a series of different titanocene DAD complexes $Cp_2Ti(R^1,R^2\text{-DAD})$ (R^1 = Ph, C_6H_4-2-Me, C_6H_4-4-Me, C_6H_4-4-OMe, 1-$C_{10}H_7$, $R^2 = Me$; **14**–**18**) have been used to estimate the energy barrier of the thermal induced inversion of the folded diazametallacyclopentene rings and to identify rotameric isomers derived from restricted rotation of the C_6H_4-2-Me and the 1-$C_{10}H_7$ group about the N–C_{ipso} bond of the DAD ligand. Accordingly, complexes **16** and **18** and also the half-sandwich complexes **3** and **13** adopt mixtures of *meso* and *rac* rotamers. Finally, the crystal structure of $Cp_2Hf(R^1,R^2\text{-DAD})$ (**21**, $R^1 = R^2 = Ph$) is reported.

Keywords: Half-sandwich complexes; 1,4-Diaza-1,3-diene complexes; *supine* Conformation

* Corresponding author. Tel.: +49-261-9119328; fax: +49-261-37524.
E-mail address: scholz@uni.koblenz.de (J. Scholz).

0022-328X/01/$ - see front matter
PII: S0022-328X(01)00705-7

1. Introduction

Recently the interest in early transition metal chemistry has been focused on Group 4 and 5 complexes that contain chelating diamide ligands [1]. Complexes with these ligands exhibit a close relationship to the metallocenes and particularly to the constrained-geometry half-sandwich amidometal complexes, which have been studied as potential catalysts for homogeneous Ziegler–Natta polymerization [2]. For example, chelating diamide complexes of titanium and zirconium serve as precursors for the highly active and living polymerization of α-olefins [3]. The potential advantage of the bis(amido)metal system relative to the metallocene or the half-sandwich amidometal complexes is their lower formal electron count which results in a more electrophilic and therefore potentially more active catalyst fragment [4].

In the last few years, several new DAD complexes (1,4-diaza-1,3-diene: $R^1N{=}CR^2CR^2{=}NR^1$ (R^1,R^2-DAD) of Group 4 and 5 elements have been synthesized by other groups [5] as well as by our group [6]. In the majority of these complexes the heterodienes are coordinated in their dianionic form as chelating enediamides to the metal (Scheme 1, σ^2-*N*,*N*′,π, **a**) and therefore are reminiscent of diamide ligands. Nevertheless, unlike the diamides the enediamide ligands exhibit further versatile coordination modes ranging from η^2-NC (**b**), μ^2-(σ^2-*N*,*N*′,π) (**c**), σ-*N*,μ^2-*N*′,η^2-CN′ (**d**), to σ,σ′-*N*,*N*′ (**e**). Most spectacular in this context is the niobium complex Nb_2(*t*-Bu,H-DAD)$_5$ whose molecular structure shows DAD ligands in three different bonding modes [7].

To get more insight into the structure–reactivity relationships of early transition metal DAD complexes we report here the syntheses, structures and details of molecular dynamics of various new DAD complexes of titanium, zirconium and hafnium.

2. Results and discussion

2.1. Syntheses of CpM(DAD)Cl complexes (M = Ti, Zr)

Previous investigations have demonstrated that the half-sandwich DAD complexes of the type CpM(DAD)Cl (M = Ti, Zr; Cp = η^5-C_5H_5) can easily be prepared by reduction of $CpTiCl_3$ or $CpZrCl_3(THF)_2$ with magnesium turnings in the presence of DAD ligands (Scheme 2) [6b,8]. The titanium complexes CpTi(R^1,R^2-DAD)Cl: **2** (R^1 = C_6H_4-4-OMe, R^2 = H), **3** (R^1 = C_6H_4-2-Me, R^2 = Me) and **5** (R^1 = C_6H_4-4-Me, R^2 = Ph) obtained in this way and described herein, form dark red crystalline solids whereas the zirconium complexes CpZr(R^1,R^2-DAD)Cl: **6** (R^1 = C_6H_4-4-OMe, R^2 = H), **7** (R^1 = C_6H_4-4-OMe, R^2 = Me) and **8** (R^1 = C_6H_4-4-Me, R^2 = Ph) which are poorly soluble in common organic solvents could be isolated as pale yellow crystalline precipitates.

The NMR spectroscopic data of the titanium complexes **2** and **5** are consistent with the presence of a mirror plane of symmetry passing through the Ti and Cl atoms and bisecting the N–Ti–N angle of the five-membered chelate ring (complex **3** will be separately discussed later). Each pair of substituents on the N atoms and the C atoms of the DAD backbone exhibits one characteristic set of ^{1}H- and ^{13}C-NMR resonances. Moreover, the ^{13}C-NMR signal of the C atoms of the DAD backbone appears in the olefinic range (**2**, δ 107.1; **5**, δ 119.5), which is an evidence for a distinct enediamide structure (Scheme 1, **a**). Furthermore, the X-ray structure analyses of **2** and **5** [9] as well as of the analogous complex **4** (R^1 = C_6H_4-4-OMe, R^2 = Me), reported earlier [6b], confirmed that the DAD ligands in all of these half-sandwich complexes adopt the *supine* conformation [10]. These results support the assumption that substituents bonded to the carbon atoms of the DAD backbone do not strongly influence the conformation geometry of CpTi(DAD)Cl complexes. On the other hand the sterical size of alkyl groups bonded to the terminal nitrogen atoms of the DAD ligand has a dramatic effect on the conformation geometry of half-sandwich DAD complexes. For instance, Tatsumi et al. have recently found that the *i*-Pr substituted DAD ligand in Cp*Ta(*i*-Pr,H-DAD)Cl_2 prefers the *supine* conformation (Scheme 3, **a**) whereas the *t*-Bu substituted DAD in Cp*Ta(*t*-Bu,H-DAD)Cl_2 exhibits the *prone* conformation (Scheme 3, **b**) [11].

The NMR spectra of the zirconium half-sandwich complexes **6**–**8** are in principle comparable with those

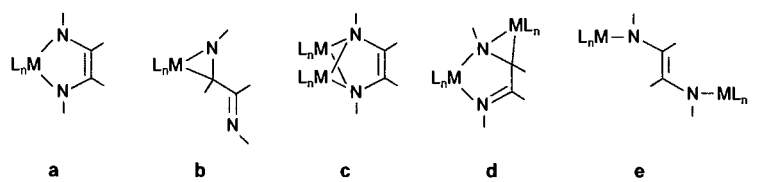

Scheme 1. Selected bonding types in enediamide complexes of early transition metals: (a) σ^2-N,N′,π; (b) η^2-NC; (c) μ^2-(σ^2-N,N′,π); (d) σ-N,μ^2-N′,η^2-CN′; and (e) σ,σ′-N,N′.

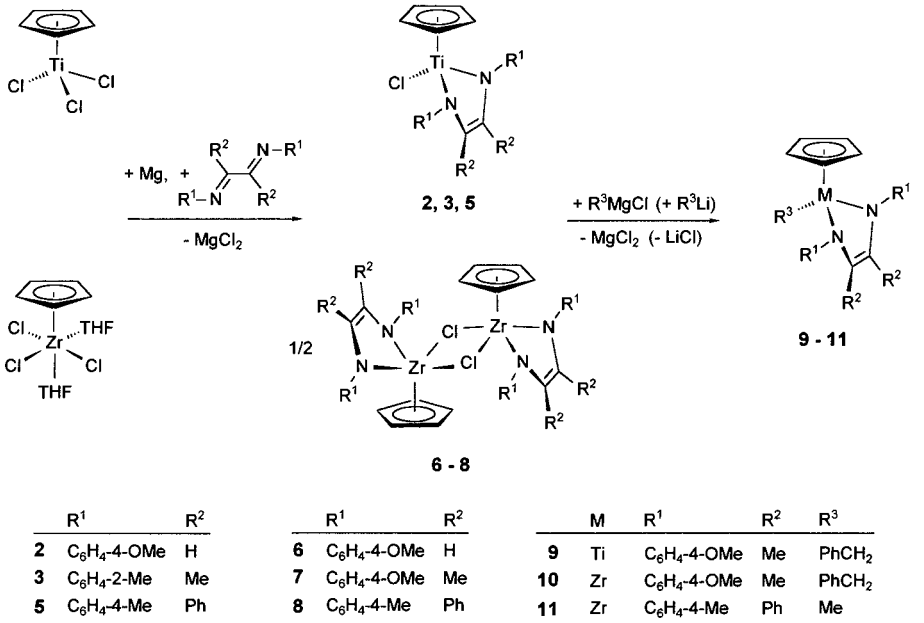

	R1	R2
2	C_6H_4-4-OMe	H
3	C_6H_4-2-Me	Me
5	C_6H_4-4-Me	Ph

	R1	R2
6	C_6H_4-4-OMe	H
7	C_6H_4-4-OMe	Me
8	C_6H_4-4-Me	Ph

	M	R1	R2	R3
9	Ti	C_6H_4-4-OMe	Me	$PhCH_2$
10	Zr	C_6H_4-4-OMe	Me	$PhCH_2$
11	Zr	C_6H_4-4-Me	Ph	Me

Scheme 2. Synthesis of the half-sandwich 1,4-diaza-1,3-diene complexes of the type CpM(DAD)Cl (M = Ti, Zr) and alkylation reaction with MeLi and $PhCH_2MgCl$.

of the titanium complexes **2** and **5**. They are also in accord with a symmetric coordination of the DAD ligands combined with a charge transfer from the zirconium to the ligand forming a distinct enediamide structure. Furthermore, on the basis of the NMR data we conclude that the DAD ligands again adopt the *supine* conformation. Unfortunately, we were not successful in preparing crystals of the zirconium complexes suitable for X-ray diffraction analysis. Nevertheless, in view of their poor solubility in nonpolar organic solvents such as toluene we assume that the complexes **6**–**8** form dimeric units by bridging chlorine atoms as was already demonstrated by the solid state structure of the complex $[CpZr(t\text{-Bu,H-DAD})Cl]_2$ [12]. As expected, these dimeric units dissociate completely in diethyl ether or THF.

Unlike the titanium half-sandwich complexes **2** and **5** the room temperature ^{1}H-NMR spectrum of **3** shows resonances for two distinct species whose relative intensities do not change from -80 to $+80$°C in toluene-d_8. These resonances are in agreement with a mixture of two rotameric isomers of **3** in solution (Scheme 4). The formation of these distinct species during the synthesis of **3** is attributed to a high barrier to rotation of the nitrogen-bonded *o*-tolyl groups about the N–C_{ipso} bond. Furthermore, it is to be expected that the *o*-tolyl groups impede to a high degree the folding of the diazametallacyclopentene ring if they are twisted in *trans*-direction (*rac*-isomer). Thus, the *meso*-isomer with *o*-tolyl groups, which are *cis*-arranged, should be more favored. Indeed, integration of the Cp signals in the ^{1}H-NMR spectrum indicates a *rac*/*meso* ratio of about 1:2.

In accord with the presence of four chemical nonequivalent methyl groups the C_2-symmetric *rac*-isomer displays four signals at δ 2.31, 1.96, 1.88, and 1.84. The remaining two prominent methyl resonances at δ 1.91 and 1.87 are readily assigned to the other rotamer, the C_2-symmetric *meso*-isomer. Naturally the existence of the two isomers of **3** in about a 1:2 ratio is also reflected by their ^{13}C-NMR spectra.

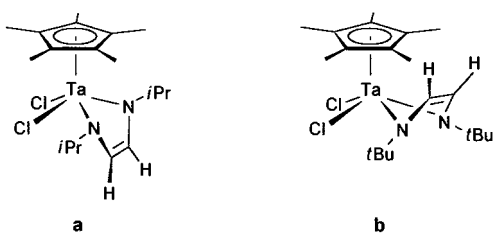

Scheme 3. Structures of half-sandwich 1,4-diaza-1,3-diene complexes of tantalum: (a) *supine*-Cp*Ta(*i*-Pr,H-DAD)Cl_2 and (b) *prone*-Cp*Ta(*t*-Bu,H-DAD)Cl_2.

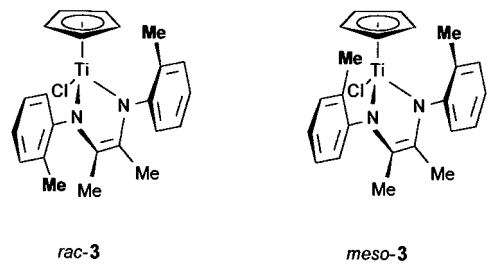

Scheme 4. Rotameric isomers of $CpTi(C_6H_4$-2-Me,Me-DAD)Cl **3**: *meso*-**3** and *rac*-**3**.

Table 1
Selected bond distances (Å) and angles (°) of **9** with estimated standard deviations in parentheses

Ti1–N1	1.907(5)	Ti1–N2	1.919(4)
Ti1–C13	2.435(5)	Ti1–C15	2.435(4)
N1–C13	1.375(5)	N2–C15	1.389(6)
C13–C15	1.383(8)	Ti1–C24	2.182(5)
N1–Ti1–N2	89.4(2)	Ti1–C24–C25	110.5(4)
Ti1–N1–C13	94.4(3)	Ti1–N2–C15	93.4(3)
N1–Ti1–C24	108.3(2)	N2–Ti1–C24	106.5(2)
(Ti1,N1,N2)-(N1,C13,C15,N2) = Θ	129.50(2)		
Sum of angles at N1	359.2(5)		
Sum of angles at N2	359.5(5)		

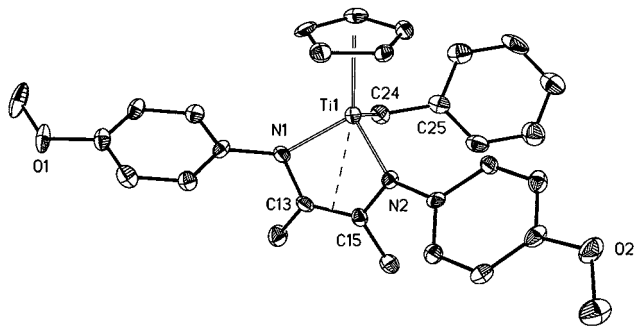

Fig. 1. Molecular structure of **9** with atomic numbering (ORTEP, 40% probability ellipsoids, hydrogen atoms omitted for clarity). Depicted is only one of the three independent molecules.

2.2. Alkylation of the half-sandwich 1,4-diaza-1,3-diene complexes CpM(DAD)Cl

Reaction of the half-sandwich titanium and zirconium chloride complexes **4** and **7** with one equivalent of $PhCH_2MgCl$ and of **8** with one equivalent of MeMgI affords the alkyl derivatives $CpM(R^1,R^2\text{-DAD})CH_2Ph$ (**9**, M = Ti, $R^1 = C_6H_4$-4-OMe, R^2 = Me; **10**, M = Zr, $R^1 = C_6H_4$-4-OMe, R^2 = Me) and $CpZr(R^1,R^2\text{-DAD})Me$ (**11**, $R^1 = C_6H_4$-4-Me, R^2 = Ph) as bright red (**9**) and yellow (**10**, **11**) crystalline solids (Scheme 2). The benzyl complexes as well as the methyl derivative are air- and moisture sensitive, but are thermally stable in the solid state and in solution. They were characterized by IR and mass spectra and their structures were determined by NMR spectroscopy and further by the crystallographic study for **9** (vide infra).

The ^{13}C resonance of the Zr–CH_3 ligand in **11** occurs at δ 20.7 ($^1J_{C-H}$ = 113.0 Hz) which is in good agreement with the analogues methyl complex $[(Me_3Si)_2C_5H_3]Zr(Ph,Me\text{-DAD})CH_3$ [8]. In the benzyl complex **9** the resonance due to the *ipso*-carbon atom of the phenyl ring at δ 157.4 and the $^1J_{C-H}$ coupling constant of the benzylic methylene group (122.0 Hz) are typical of an η^1-bonded benzyl ligand [13]. Furthermore, the NMR resonances of the DAD ligands both of the benzyl complexes and of the methyl derivative do not differ significantly from those of the precursor complexes **4**, **7** or **8**. Thus, during the alkylation reactions leading to **9**, **11** and **12**, the *supine* orientation of the DAD ligands is maintained.

2.3. Crystal structure of $CpTi[N(C_6H_4\text{-}4\text{-}OMe)C(Me)=C(Me)N(C_6H_4\text{-}4\text{-}OMe)]CH_2Ph$ (9)

The molecular structure determination of **9** provides the opportunity to evaluate the structural consequences resulting from the substitution of the chlorine atom in **4** by an alkyl group, in this case CH_2Ph. Recrystallization of the benzyl complex **9** from diethyl ether gave red single crystals appropriate for an X-ray diffraction determination (Table 1 and Section 4). The unit cell of **9** contains three independent molecules with very similar geometrical parameters. A perspective view of the structure of one of the molecules is shown in Fig. 1.

Complex **9** is tetracoordinated by a η^5-bonded cyclopentadienyl ligand, a η^1-bonded benzyl group and the two nitrogen atoms of the symmetrically chelating DAD ligand. Furthermore, as it was concluded from the NMR spectra the heterodiene is coordinated in the *supine* conformation. In contrast, Mashima et al. have recently reported that during the dialkylation of the tantalum complex $Cp^*Ta(C_6H_4\text{-}4\text{-}OMe,H\text{-DAD})Cl_2$ with $Mg(CH_2Ph)_2$ a change of the DAD coordination geometry from the *supine* conformation to the *prone* one takes place [5o]. The C13–C15 distance of the DAD backbone in **9** (1.383(8) Å) is significantly shortened compared with that of a free DAD ligand such as C_6H_4-4-Me,Me-DAD (1.499(12) Å) [14]. In addition, the N1–C13 (1.375(5) Å) and N2–C15 (1.389(6) Å) distances are accordingly longer than those found for C_6H_4-4-Me,Me-DAD (1.288(7) Å) [14]. Thus, these structural data are ample proof that the DAD ligand, as in the precursor complex **4**, is double reduced into the enediamide form generating an 1,3-diaza-2-titanacyclopentene ring. The five-membered ring is folded along the N–N vector by an angle of 129.5(2)° which however is considerably larger than in the chloride complex **4** (Θ = 119.50(6)° [6b]. Nevertheless, the distances Ti–C13 (2.435(5) Å) and Ti–C15 (2.435(4) Å) are short enough for the titanium atom to interact with the π-bonding system of the olefinic carbon atoms C13 and C15 of the enediamide ligand [5c]. However, Mealli et al. reported recently that the π component of the σ^2,π-enediamide structure (Scheme 1, **a**) also can be largely contributed by the two nitrogen σ lone pairs [15]. The planar sp^2 bonding geometry at the nitrogen atoms (sum of angles: N1 359.2(5)°, N2 359.5(5)°) agrees with this bonding description, but the Ti–N bonds are not appreciably shortened.

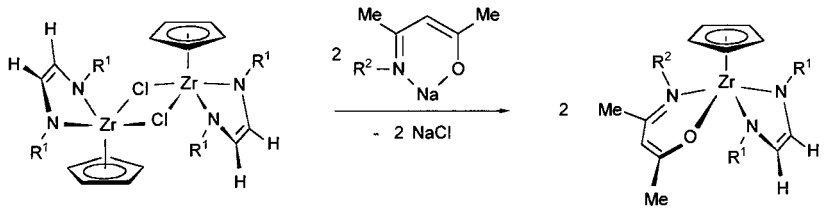

Scheme 5. Reaction of $CpZr(C_6H_4$-4-OMe,H-DAD)Cl (**6**) with Na[$(C_6H_4$-4-Me)N=C(Me)CH=C(Me)O].

An important characteristic of benzyl groups is their ability to interact in an η^n ($n = 2 - 6$) fashion to electron deficient metal centers. In the case of high valent, early *d*-block metals' multisite bonding of benzyl ligands to the electron deficient metal center has been established in a number of cases, typically with M–CH_2–Ph angles of less than 100° and a close contact between the *ipso*-carbon atom of the phenyl group and the metal center [13,16]. However, the open bond angle Ti1–C24–C25 of 110.5(4)° in **9** indicates strict η^1-benzyl coordination as was found in other titanium benzyl complexes, e.g. $Cp_2Ti(CH_2Ph)_2$ [13] and $Cp^*Ti(CH_2Ph)_3$ [17]. Moreover, the η^1-coordination mode of the benzyl group in **9** suggests that the metal center should have no appreciable electron deficiency.

2.4. Reaction of [CpZr(DAD)Cl]$_2$ with sodium acetylacetoneiminate

Treatment of the half-sandwich zirconium complex **6** with the sodium salt of the Schiff base acetylacetone-*p*-tolylimine Na[$(C_6H_4$-4-Me)N=C(Me)CH=C(Me)O] (Na[N⌒O]) in THF affords the new zirconium complex **12** in 83% yield as shown in Scheme 5. Complex **12** was isolated and stored as a relatively stable yellow crystalline solid that decomposes slowly by prolonged exposure to air. Satisfactory crystals were obtained by repeated recrystallization from diethyl ether at -30°C.

The spectroscopic data of **12** are straightforward, the ^{1}H-NMR spectrum in THF-d_8 exhibits one set of signals due to both the DAD and acetylacetoneiminate ligand in a 1:1 integral ratio, consistent with the proposed structure. Additionally, the ^{1}H-NMR spectrum displays independent signals for each of the inner protons of the DAD ligand (δ 5.92 and 5.62) as well as of the methyl groups of the C_6H_4-4-OMe substituents at the N atoms (δ 3.72 and 3.68) indicating that the heterodiene is in an unsymmetric environment. The N,O-bonded acetylacetoneiminate ligand OC(*Me*)=C*H*C(*Me*)=N(C_6H_4-4-*Me*) gives rise to one singlet for the methine proton (δ 5.05) and three signals for the methyl protons (δ 2.19, 1.69 and 1.48). The aromatic region of the ^{1}H-NMR spectrum is more complex and displays four doublets for the protons of the two nonequivalent C_6H_4-4-OMe groups and four other doublets for each of the aromatic protons of the C_6H_4-4-Me group. The nonequivalence of these protons reflects restricted rotation on the NMR time scale of this *p*-tolyl ring about the C–N bond.

The molecular structure of **12** in the solid state was determined by an X-ray diffraction study and is presented in Fig. 2, while pertinent bonding parameters are given in Table 2. Crystal structure and refinement data are summarized in Section 4. The zirconium atom is pentacoordinated by the Cp group, the DAD and the chelating acetylacetoneiminate ligand. As expected the double reduced heterodiene is bound in the *supine* conformation forming a 1,3-diaza-2-zirconacyclopentene ring whose folding ($\Theta = 119.1(1)$°) moves the internal carbons, C1 and C2, closer to the electrophilic zirconium center (2.509(3) Å). The six membered acetylacetoneiminate ring is nearly planar, displacements from this plane of O3 and N3 atoms are 0.136 and 0.087 Å, respectively. The angle between the chelate ring and the plane defined by the carbon atoms of the Cp ring is about 34.1°. The bonding parameters Zr–O3 (2.133(2) Å), Zr–N3 (2.343(2) Å), Zr–O3–C19 (137.4(2)°) and Zr–N3–C17 (129.0(2)°) as well as the other bond distances and angles within the acetylace-

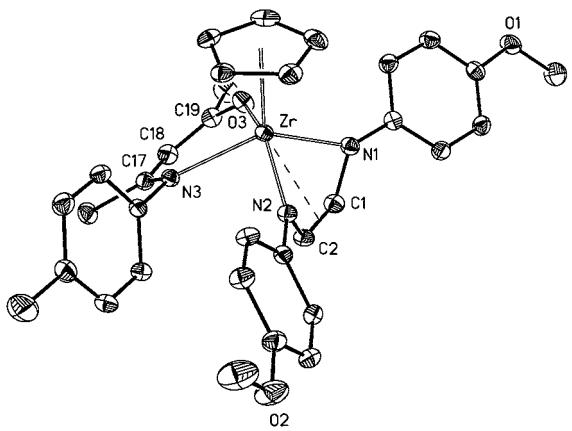

Fig. 2. Molecular structure of **12** with atomic numbering (ORTEP, 40% probability ellipsoids, hydrogen atoms omitted for clarity).

Table 2
Selected bond distances (Å) and angles (deg) of **12** with estimated standard deviations in parentheses

Zr–N1	2.106(2)	Zr–C1	2.509(3)
Zr–N2	2.107(2)	Zr–C2	2.509(3)
N1–C1	1.387(3)	N2–C2	1.389(3)
C1–C2	1.366(3)		
Zr–N3	2.343(2)	N3–C17	1.319(3)
Zr–O3	2.133(2)	O3–C19	1.284(3)
C17–C18	1.423(4)	C18–C19	1.354(4)
N1–Zr–N2	81.88(8)	N1–Zr–N3	131.74(7)
N2–Zr–N3	87.21(7)	N1–Zr–O3	84.20(8)
N2–Zr–O3	142.56(8)	N3–Zr–O3	76.64(7)
Zr–O3–C19	137.4(2)	Zr–N1–C1	89.3(1)
Zr–N2–C2	89.3(1)	Zr–N3–C17	129.0(2)
(N1,C1,C2,N2)-(Zr,N1,N2) = Θ	119.1(1)		
(N1,C1,C2,N2)(C3–C8)	49.2(1)		
(N1,C1,C2,N2)(C10–C15)	43.2(1)		
Sum of angles at N1	352.5(3)		
Sum of angles at N2	358.3(3)		
Sum of angles at N3	360.0(3)		

toneiminate ring fall well within the range observed for other acetylacetoneiminate zirconium [18] or lanthanum [19] complexes, indicating a rigid behavior of this type of ligand.

2.5. Hydrolysis of CpTi(DAD)Cl

In the course of our work on half-sandwich titanium DAD complexes CpTi(DAD)Cl we observed that these compounds are somewhat sensitive towards moisture. Consequently, controlled hydrolysis of the half-sandwich titanium complex **3** (*rac*/*meso* = 1:2) was performed by employing the base imidazole [20] and one equivalent of water. The reaction results in the formation of the dark red, oxo-bridged dimeric complex **13** in about 80% yield (Scheme 6).

In spite of the large molecular weight of 770.69 g mol^{-1} the molecule ion [M$^+$] of complex **13** is observed in the EI-MS spectrum with 100% relative intensity. Moreover, there is evidence in the ^{1}H- and ^{13}C-NMR spectra of **13** for three isomeric species, *meso*/*meso*-**13**, *meso*/*rac*-**13** and *rac*/*rac*-**13**, being present in solution and arising from different combinations of the two rotamers *rac*-**3** and *meso*-**3** after hydrolysis. For example, the ^{1}H-NMR spectrum shows a very intensive single resonance at δ 5.96 caused by the two equivalent Cp ligands of the *meso*/*meso*-isomer, two distinct resonances of equal intensity at δ 5.95 and 5.88 which can be assigned to the two nonequivalent Cp ligands of the *meso*/*rac*-isomer and a very weak Cp resonance at δ 5.81 indicating that the *rac*/*rac*-isomer has been formed too. Comparing the intensities of these Cp resonances a ratio of the three isomeric species *meso*/*meso*-**13**:*meso*/*rac*-**13**:*rac*/*rac*-**13** of about 80:15:5 can be deduced.

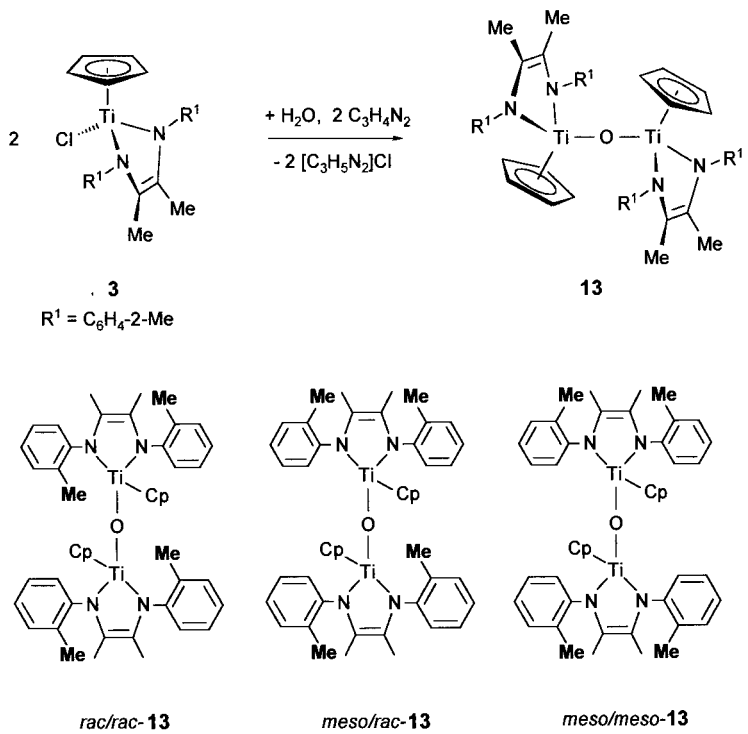

Scheme 6. Hydrolysis of the half-sandwich titanium complex CpTi(C_6H_4-2-Me,Me-DAD)Cl (**3**).

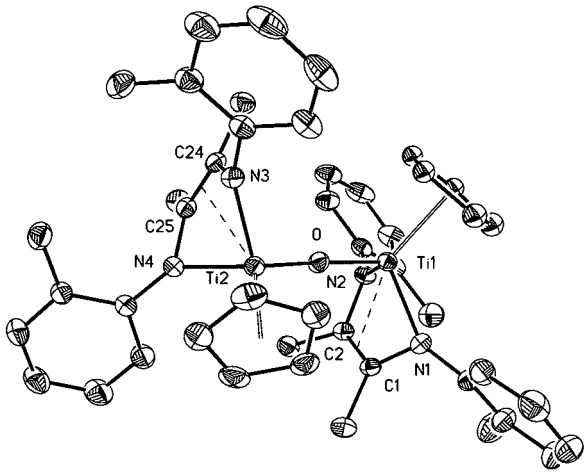

Fig. 3. Molecular structure of *meso*/*meso*-**13** with atomic numbering (ORTEP, 40% probability ellipsoids, hydrogen atoms omitted for clarity).

Table 3
Selected bond distances (Å) and angles (°) of **13** with estimated standard deviations in parentheses

Ti1–N1	1.947(3)	Ti1–N2	1.930(3)
Ti1–C1	2.464(4)	Ti1–C2	2.477(4)
N1–C1	1.385(5)	N2–C2	1.398(4)
C1–C2	1.366(5)	Ti1–O	1.817(2)
Ti2–N3	1.946(3)	Ti2–N4	1.924(3)
Ti2–C24	2.425(4)	Ti2–C25	2.425(4)
N3–C24	1.402(5)	N4–C25	1.393(5)
C24–C25	1.375(5)	Ti2–O	1.836(2)
N1–Ti1–N2	87.1(1)	N3–Ti2–N4	87.4(1)
Ti1–N1–C1	93.8(2)	Ti2–N3–C24	91.4(2)
Ti1–N2–C2	94.9(2)	Ti2–N4–C25	92.4(2)
Ti1–O–Ti2	169.6(2)	Cp–Ti1–Ti2–Cp′	77.5(2)
(N1,C1,C2,N2)-(Ti1,N1,N2) = Θ		128.5(2)	
(N3,C24,C25,N4)-(Ti2,N3,N4) = Θ		123.7(2)	
Sum of angles at N1	357.7(5)		
Sum of angles at N2	359.8(5)		
Sum of angles at N3	357.9(5)		
Sum of angles at N4	357.6(5)		

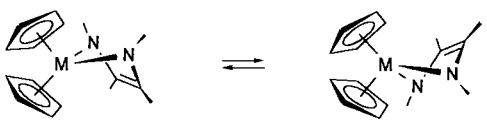

Scheme 7. Dynamic equilibrium between the two folded ring conformations of metallocene DAD complexes.

The solid state structure of the major isomer *meso*/*meso*-**13** was also confirmed by X-ray diffraction. The molecule structure and atom numbering scheme of *meso*/*meso*-**13** is given in Fig. 3, selected bond distances and angles are listed in Table 3. A π-bonded Cp ring and a *supine*-coordinated DAD ligand are bound to each of the two titanium atoms which are linked by a single oxygen atom.

The Ti–O bond distances were found to be 1.817(2) and 1.836(2) Å. These are similar in length to the Ti–O bond distances found in $[CpTi(SCH_2CH_2CH_2S]_2O$ (1.80(1) and 1.81(1) Å, one of the two crystal forms) [20] but significantly shorter than those found in titanium alkoxides, such as $Cp_2Ti(OC_2H_3)_2$ (1.903(2) Å) or $Cp_2TiCl(OC_2H_5)$ (1.885(2) Å) [21]. Additionally, the Ti1–O–Ti2 angle (169.6(2)°) compares well with the linear moiety found in $(CpTiCl_2)_2O$ [22] or the nearly linear moiety in $[CpTi(SCH_2CH_2CH_2S]_2O$ (166.0(7)°) [20]. The relative short Ti–O distances and the large Ti1–O–Ti2 angle are consistent with π-bonding between the titanium and oxygen atoms. Interestingly, the position of the DAD ligands about the Ti1–O–Ti2 vector is such, that the Cp rings are approximately orthogonal (Cp–Ti1–Ti2–Cp′ 77.5°). This arrangement allows the effective interaction of vacant d-orbitals on each titanium atom with one pair of electrons on the bridging oxygen atom, affording the significant Ti–O π-bonding [20]. As expected from the NMR spectra, the nitrogen-bonded *o*-tolyl groups are twisted in *cis*-direction (*meso*-isomer) which enables the five-membered chelate rings to be folded along the N–N vector by an angle of 128.5(2) and 123.7(2)°, respectively.

2.6. Structures and molecular dynamics of metallocene(DAD) complexes

A notable structural feature associated with the molecular structures of the DAD complexes of the early transition metals is their distinct lack of planarity of the 1,3-diaza-2-metallacyclopentene ring. In the case of metallocene DAD complexes Cp_2M(Ph,R-DAD) (M = Ti; R = Me (**14**), Ph (**19**); M = Zr, R = Ph (**20**)) already published, the folding along the N–N line segment of the chelate ring therefore results in the two Cp ligands becoming nonequivalent [6a]. However, in solution the ^{1}H-NMR spectra of these complexes at ambient temperatures indicate the presence of only one type of Cp ligand. Hence we concluded that the complexes are very fluxional on the NMR time scale involving rapid dynamic equilibrium between two nonequivalent folded ring conformations as depicted in Scheme 7.

To provide more insight into this dynamic equilibrium and to learn about the influence of substituents bound to the heterodiene we investigated some new titanocene complexes Cp_2Ti(R,Me-DAD) (R = C_6H_4-4-Me (**15**), C_6H_4-2-Me (**16**), C_6H_4-4-OMe (**17**), 1-$C_{10}H_7$

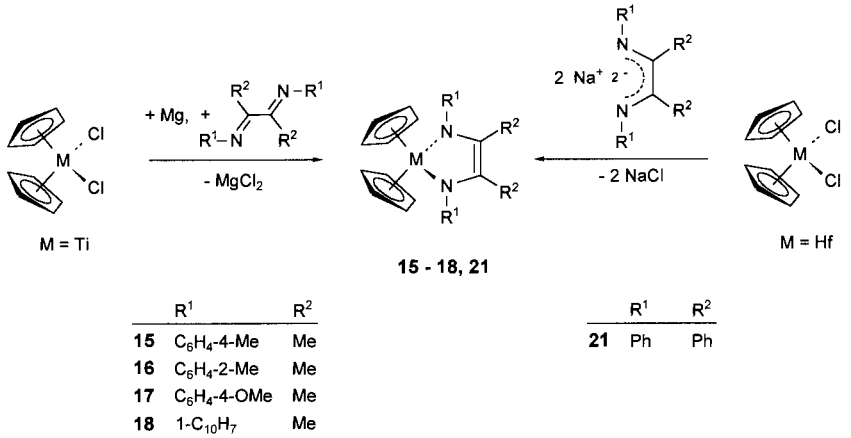

Scheme 8. Syntheses of the metallocene complexes Cp_2Ti(R,Me-DAD), R = C_6H_4-4-Me (**15**), C_6H_4-2-Me (**16**), C_6H_4-4-OMe (**17**), and 1-$C_{10}H_7$ (**18**) and of Cp_2Hf(Ph,Ph-DAD) (**21**).

(**18**)). Furthermore we completed the series of the metallocene benzildianil complexes **19** and **20** [6a] by the hafnium derivative Cp_2Hf(Ph,Ph-DAD) **21**.

The new titanocene complexes Cp_2Ti(R,Me-DAD) are readily prepared by reduction of Cp_2TiCl_2 with magnesium turnings in the presence of the DAD ligands **1c**–**1f** in THF as already published for the analogous derivative Cp_2Ti(Ph,Me-DAD) **14** (Scheme 8) [6a]. Reaction of Cp_2HfCl_2 with the disodium compound of **1g** affords the orange complex **21**.

Solid state structural analysis of **21** (Fig. 4, Table 4) shows a puckering of the diazametallacyclopentene ring ($\Theta = 149.5(4)°$) which is somewhat larger than those of the analogous zirconium complex **20** ($\Theta = 140.2(2)°$, average value). However, the other bond distances and angles are almost identical with those of **20**.

At ambient temperatures the ^{1}H-NMR spectra of **21** as well as of the titanocene complexes **15** and **17** indicate the presence of only one type of Cp ligand. As expected, on lowering the temperature the Cp signal of the metallocene unit of these complexes broadens, then decoalesces, and finally gives rise to distinct resonances for both of the Cp ligands. The final, limiting low temperature spectra are fully consistent with the observed solid state structure of **21** or other known metallocene DAD complexes of Group IVa metals [5o,6a,13].

Analysis of the NMR spectra allows one to estimate the activation energy for the ring inversion at the coalescence temperature T_c. Table 5 lists the values of $\Delta G^{\#}$ for this dynamic process estimated from the coalescence temperatures T_c. A comparison of the inversion barriers for **14**, **15** and **17** with that for **19**–**21** indicates that substituents on the carbon backbone of the DAD ligands do not seem very important for the rate of this degeneration process. Moreover, the activation barriers determined for our metallocene DAD complexes correspond largely to the values of $\Delta G^{\#}$ for the ring inversion reported for other nonplanar DAD complexes of Group 4 metals [5c].

The room temperature NMR spectra of the titanocene complexes **16** and **18** are markedly different from those of the titanocene complexes reported above and show two complete sets of resonances each. As in

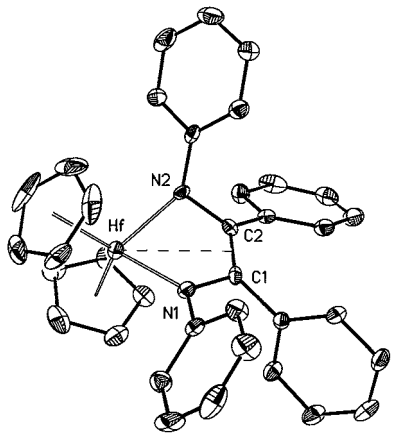

Fig. 4. Molecular structure of **21** with atomic numbering (ORTEP, 40% probability ellipsoids, hydrogen atoms omitted for clarity).

Table 4
Selected bond distances (Å) and angles (°) of **21** with estimated standard deviations in parentheses

Hf–N1	2.102(5)	Hf–N2	2.080(5)
Hf–C1	2.785(6)	Hf–C2	2.786(6)
N1–C1	1.392(7)	N2–C2	1.420(7)
C1–C2	1.384(8)		
N1–Hf–N2	79.5(2)	Cp–Hf–Cp	129.0(2)
Hf–N1–C1	103.8(3)	Hf–N2–C2	102.9(3)
(N1,C1,C2,N2)(N1,Hf,N2) = Θ	149.5(4)		
(N1,C1,C2,N2)(C3···C8)	103.1(4)		
(N1,C1,C2,N2)(C9···C14)	34.9(4)		
(N1,C1,C2,N2)(C15···C20)	104.2(4)		
(N1,C1,C2,N2)(C21···C26)	107.8(4)		
Sum of angles at N1	360.0(7)		
Sum of angles at N2	357.2(7)		

Table 5
Estimated barriers for the ring inversion of the metallocene DAD complexes **14**–**21** [a]

Solvent	**14** [b] CD_2Cl_2	**15** CD_2Cl_2	*rac*-**16** [c] Toluene-d_8	**17** CD_2Cl_2	*rac*-**18** [d] Toluene-d_8	**19** [b] CD_2Cl_2	**20** [b] CD_2Cl_2	**21** CD_2Cl_2
T_c (°C) [e]	−18	±0	+57	−8	+51	−4	+10	+1
$\Delta\nu$ (Hz) [f]	12	12	35	8	99	84	92	102
$\Delta G_T^{\#}$ (kJ mol^{-1})	55.2(±1)	59.2(±1)	69.1(±1)	58.2(±1)	65.0(±1)	53.8(±1)	56.7(±1)	54.5(±1)

[a] Estimated by temperature dependent NMR spectroscopy.
[b] Ref. [5a].
[c] Coalescence of the Me group signal N(C_6H_4-2-*Me*): $T_c = +61$°C, $\Delta\nu = 42$ Hz, $\Delta G_T^{\#} = 69.2(\pm 1)$ kJ mol^{-1}; coalescence of the Me group signal =C(*Me*): $T_c = +53$°C, $\Delta\nu = 25$ Hz, $\Delta G_T^{\#} = 69.1(\pm 1)$ kJ mol^{-1}.
[d] Coalescence of the Me group signal =C(*Me*): $T_c = +42$°C, $\Delta\nu = 52$ Hz, $\Delta G_T^{\#} = 64.8(\pm 1)$ kJ mol^{-1}.
[e] Coalescence temperature of the Cp group signal.
[f] Difference of the chemical shift of the Cp signals in the limiting low-temperature spectrum.

the case of the half-sandwich titanium complex **3** the one-pot synthesis of the titanocene complexes **16** and **18** also leads to a *rac*/*meso*-mixture of diastereoisomers again but in contrast to the half-sandwich complex **3** with a considerable higher yield of the *rac*-isomer (**16**, *rac*/*meso* ≈ 10:1; **18**, *rac*/*meso* ≈ 8:1). A stacked plot of a portion of the ^{1}H-NMR spectrum (methyl region) of *rac*/*meso*-**18** at several temperatures is shown in Fig. 5.

At room temperature the Cp protons of the *rac*-isomer give rise to singlets at δ 5.64 and 5.22 and the methyl protons show singlets at δ 1.68 and 1.51, respectively. The Cp resonances of the *meso*-isomer appear at δ 5.44 and 5.25, and the methyl protons are observed at δ 1.55. Interestingly, on warming only the Cp and the methyl group signals of *rac*-**18** broaden further and then coalesce. At the coalescence temperature of the Cp resonances, T_c of 51°C, an approximate value of $\Delta G^{\#}$ for this inversion process was calculated to be 65.0(±1) kJ mol^{-1}, which is rather high when compared with the values obtained for **14**, **15** and **17**. As expected, the value of the activation energy for the ring inversion estimated at the coalescence temperature of the methyl protons ($T_c = 38$°C, $\Delta G^{\#} = 64.8(\pm 1)$ kJ mol^{-1}, Fig. 5) does not differ from that of the Cp coalescence.

The high-temperature limiting spectrum (+85°C) only shows one sharp singlet for both of the Cp groups and one resonance for the methyl protons, respectively, suggesting that the inversion of the folded 1,3-diaza-2-titanacyclopentene ring becomes rapid on the NMR time scale now. There is no doubt that the remarkably high activation energy of the ring inversion of *rac*-**18** can be attributed to a lower rate of the pyramidal inversion of the terminal nitrogen atoms which again is inhibited by the restricted rotation of the 1-naphthyl groups about the N–C_{ipso} bonds [23]. Furthermore, the set of variable-temperature ^{1}H-NMR spectra revealed that no change of the Cp group signals is observed for *meso*-**18** upon heating to 85°C. Hence, we conclude that the degree of steric hindrance in this rotameric isomer is still higher than in the *rac*-isomer and therefore precludes any rotation of the 1-naphthyl groups about the N–C_{ipso} bonds. In other words, complex *meso*-**18** exhibits a static, nonplanar geometry of the 1,3-diaza-2-titanacyclopentene ring with Cp groups becoming diastereotopic. An identical situation was found for the *rac*/*meso* mixture of the titanocene complex **16** [24]. Currently we are trying to isolate the *rac*- as well as the *meso*-isomer of **16** or **18** from their mixtures in order to determine their solid-state structures and to demonstrate that the origin of their different dynamic behavior is in fact caused by geometrical parameters.

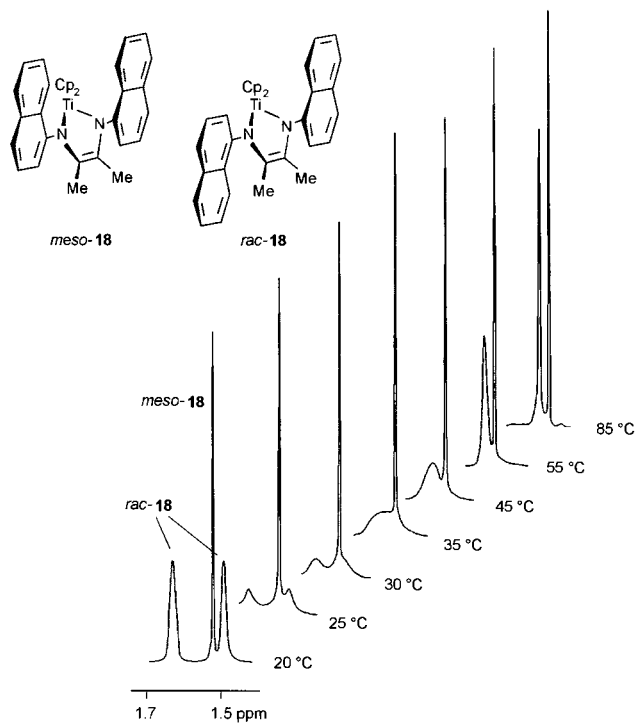

Fig. 5. ^{1}H-NMR spectra of **18** at various temperatures (methyl region, toluene-d_8, $T = 20$ to 85°C).

3. Conclusions

In this contribution, we have synthesized and characterized various new mono- and bis(η^5-cyclopentadienyl)titanium, zirconium and hafnium complexes bearing a DAD ligand. It turned out that the heterodienes are generally coordinated as dianionic enediamides forming a 1,3-diaza-2-metallacyclopentene ring whose most notable structural feature is the distinct lack of planarity. Furthermore, on the basis of NMR spectral data we concluded that the DAD ligands of the half-sandwich titanium and zirconium complexes always adopt the *supine* conformation, which was further confirmed by X-ray diffraction studies.

Importantly, we document one type of conformational complexity that exist for DAD complexes with bulky substituents at the nitrogen atoms in particular aryl groups such as *o*-tolyl and 1-naphthyl. NMR spectra of these complexes show resonances for two distinct species indicating a mixture of two rotameric isomers in solution. The formation of these isomers is attributed to a high barrier to rotation of the nitrogen-bonded groups about the N–C bond. Furthermore, we established that complexes with a large folding angle of the diazametallacyclopentene ring such as half-sandwich DAD complexes prefer the *meso*-isomer with N-bonded aryl groups being *cis*-directed. On the other hand metallocene DAD complexes which show a lower folding angle of the diazametallacyclopentene ring favor the *trans*-direction of the aryl groups (*rac*-isomer). In solution the metallocene DAD complexes are very fluxional on the NMR time scale involving rapid dynamic equilibrium between two nonequivalent folded ring conformations. Interestingly, the activation barrier of the ring inversion is determined by the rate of the pyramidal inversion of the nitrogen atoms which again requires the free (unhindered) rotation of the nitrogen substituents about the N–C bonds.

4. Experimental

4.1. General considerations

All operations described herein were performed under an atmosphere of purified argon in standard Schlenk-type glassware. Argon was purified by passage over reduced manganese/titanium-catalysts and activated 4 Å molecular sieves. Solvents were distilled from sodium–benzophenone ketyl (THF, diethyl ether, toluene) or CaH_2 (pentane, dichlormethane) under argon and stored over activated 4 Å molecular sieves. Deuterated solvents were dried over sodium (toluene-d_8, THF-d_8) or P_4O_{10} (CH_2Cl_2-d_2, $CHCl_3$-d) and distilled under argon before use. All glassware was thoroughly oven-dried or flame-dried under vacuum prior to use. NMR spectra were recorded on a Bruker 200 WP (^{1}H-NMR at 200.132 MHz), a Varian 300 BB (^{1}H-NMR at 300.075 MHz, ^{13}C-NMR at 75.462 MHz) or a Varian UNITY 500 spectrometer (^{1}H-NMR at 499.843 MHz, ^{13}C-NMR at 125.639 MHz) at 20 or 25°C, unless indicated otherwise. ^{1}H- and ^{13}C-NMR spectra were referenced internally using the residual solvent resonances (THF-d_8, δ_H 1.73, δ_C 25.2; toluene-d_8, δ_H 2.03, δ_C 20.4; $CHCl_3$-d, δ_H 7.23, δ_C 77.0; CH_2Cl_2-d_2, δ_H 5.32, δ_C 53.5). $^1J_{C-H}$ values were obtained from gated $\{^1H\}^{13}$C-NMR spectra. IR spectra were recorded as KBr-pellets or as Nujol mulls between KBr plates on a Nicolet 5 DXC and a Bruker IFS-66 FTIR spectrometer in the range 4000–400 cm^{-1}, and data are quoted in wavenumbers (v, cm^{-1}). MS studies were performed on an Intectra AMD 402 instrument with 70 eV electron impact ionization (EI). Elemental analyses were carried out by the analysis laboratory of this department. Melting points are uncorrected.

Literature Preparations. $CpTiCl_3$ [25a], $CpZrCl_3$ [25b], Cp_2TiCl_2 [25c], and Cp_2HfCl_2 [25d] were synthesized according to published procedures. The *N*,*N*-disubstituted 1,4-diaza-1,3-dienes **1a**–**1h** were prepared by literature methods 26. The syntheses of **4** [6b], **14**, **19** and **20** [6a] have been published elsewhere.

4.2. Crystal structure determinations

The intensity data for the compounds **9**, **12** and **13** were collected on a Nonius CAD4 diffractometer and for the compound **21** on a STOE STADI4 diffractometer, using graphite-monochromated Mo–K_α radiation. Data were corrected for Lorentz and polarization effects, but for absorption only for **21** [27,28]. The structures were solved by direct methods (SHELXS [29]) and refined by full-matrix least-squares techniques against F_o^2 (SHELXL-97 [30]). The hydrogen atoms of the compounds were included at calculated positions with fixed thermal parameters. All nonhydrogen atoms were refined anisotropically [30]. XP (SIEMENS Analytical X-ray Instruments, Inc.) was used for structure representations.

Crystal data for **9**: $C_{30}H_{32}N_2O_2Ti$, $M_r = 500.46$ g mol^{-1}, dark-red cubes, size $0.41 \times 0.31 \times 0.31$ mm^3, triclinic, space group $P1$, $a = 17.879(2)$, $b = 21.986(3)$, $c = 10.614(2)$ Å, $\alpha = 100.62(3)$, $\beta = 104.15(2)$, $\gamma = 76.08(3)°$, $V = 3889(2)$ Å^3, $T = -60$°C, $Z = 6$, $\rho_{calcd} = 1.563$ g cm^{-3}, $\mu(Mo-K_\alpha) = 3.34$ cm^{-1}, $F(000) = 948$, 10 371 reflections in $h(0/19)$, $k(-23/23)$, $l(-11/11)$, measured in the range $1.00° \leq \Theta \leq 25.00°$, 9098 independent reflections, $R_{int} = 0.064$, 7126 reflections with $F_o > 4\sigma(F_o)$, 1273 parameters, 0 restraints, $R1_{obs} = 0.056$, $wR2_{obs} = 0.039$, $R1_{all} = 0.089$, $wR2_{all} = 0.102$, GOOF = 1.220, largest difference peak and hole: 0.420/ −0.380 e Å^{-3}.

Crystal Data for **12**: $C_{33}H_{35}N_3O_3Zr$, $M_r = 612.86$ g mol^{-1}, yellow-brown prisms, size $0.48 \times 0.41 \times 0.12$ mm^3, monoclinic, space group $P2_1/n$, $a = 18.007(3)$, $b = 8.066(1)$, $c = 21.013(1)$ Å, $\beta = 101.97(1)°$, $V = 2985.7(6)$ Å^3, $T = 20°C$, $Z = 4$, $\rho_{calcd} = 1.363$ g cm^{-3}, $\mu(Mo-K_\alpha) = 4.06$ cm^{-1}, $F(000) = 1272$, 6979 reflections in $h(-23/22)$, $k(0/10)$, $l(0/27)$, measured in the range $1.36° \leq \Theta \leq 27.41°$, 6797 independent reflections, $R_{int} = 0.014$, 5365 reflections with $F_o > 4\sigma(F_o)$, 369 parameters, 0 restraints, $R1_{obs} = 0.034$, $wR2_{obs} = 0.0843$, $R1_{all} = 0.055$, $wR2_{all} = 0.092$, GOOF = 1.022, largest difference peak and hole: 0.333/−0.315 e Å^{-3}.

Crystal data for **13**: $C_{46}H_{50}N_4OTi_2$, $M_r = 770.70$ g mol^{-1}, dark-red prisms, size $0.44 \times 0.36 \times 0.20$ mm^3, triclinic, space group $P1$, $a = 10.426(1)$, $b = 13.485(2)$, $c = 16.250(2)$ Å, $\alpha = 67.60(1)$, $\beta = 77.69(1)$, $\gamma = 88.66(1)°$, $V = 2059.5(4)$ Å^3, $T = 20°C$, $Z = 2$, $\rho_{calcd} = 1.243$ g cm^{-3}, $\mu(Mo-K_\alpha) = 4.26$ cm^{-1}, $F(000) = 812$, 7529 reflections in $h(-12/12)$, $k(-14/16)$, $l(0/19)$, measured in the range $1.64° \leq \Theta \leq 25.00°$, 7247 independent reflections, $R_{int} = 0.016$, 5264 reflections with $F_o > 4\sigma(F_o)$, 429 parameters, 0 restraints, $R1_{obs} = 0.057$, $wR2_{obs} = 0.156$, $R1_{all} = 0.089$, $wR2_{all} = 0.176$, GOOF = 1.022, largest difference peak and hole: 0.547/−0.393 e Å^{-3}.

Crystal data for **21**: $C_{36}H_{30}N_2Hf$, $M_r = 669.11$ g mol^{-1}, yellow prisms, size $0.26 \times 0.18 \times 0.16$ mm^3, monoclinic, space group $P2_1/n$, $a = 8.4675(6)$, $b = 19.839(1)$, $c = 18.739(2)$ Å, $\beta = 96.717(6)°$, $V = 3126.3(4)$ Å^3, $T = 20°C$, $Z = 4$, $\rho_{calcd} = 1.422$ g cm^{-3}, $\mu(Mo-K_\alpha) = 33.61$ cm^{-1}, ψ-scan, transmin: 0.56, transmax: 0.86, $F(000) = 1328$, 7549 reflections in $h(-11/11)$, $k(0/25)$, $l(-24/24)$, measured in the range $2.05° \leq \Theta \leq 27.50°$, 6475 independent reflections, $R_{int} = 0.026$, 5008 reflections with $F_o > 4\sigma(F_o)$, 353 parameters, 0 restraints, $R1_{obs} = 0.036$, $wR2_{obs} = 0.119$, $R1_{all} = 0.055$, $wR2_{all} = 0.133$, GOOF = 1.143, largest difference peak and hole: 1.470/−0.788 e Å^{-3}.

4.3. Spectroscopic data for the 1,4-diaza-1,3-dienes **1a**–**1h** (^{1}H-NMR, 200 MHz, $CHCl_3$-d; ^{13}C-NMR, 50.1 MHz, $CHCl_3$-d)

(C_6H_4-4-OMe)N=CHCH=N(C_6H_4-4-OMe) ***(1a)***: ^{1}H-NMR: δ 8.39 (s, 2H, N=CH), 7.31 (d, 4H, $^3J_{H-H} = 8.8$ Hz, C_6H_4-4-OMe), 6.92 (d, 4H, $^3J_{H-H} = 8.8$ Hz, C_6H_4-OMe), 3.81 (s, 6H, C_6H_4-O*Me*). ^{13}C-NMR: δ 159.70 (C_6H_4-4-OMe), 157.51 (HC=N), 142.99, 122.96, 114.54 (C_6H_4-4-OMe), 55.44 (C_6H_4-4-O*Me*).

(C_6H_4-4-Me)N=C(Me)C(Me)=N(C_6H_4-4-Me) ***(1c)***: ^{1}H-NMR: δ 7.09 (d, 4H, $^3J_{H-H} = 8.3$ Hz, C_6H_4-4-Me), 6.61 (d, 4H, $^3J_{H-H} = 8.1$ Hz, C_6H_4-4-Me), 2.27 (s, 6H, C_6H_4-4-*Me*), 2.08 (s, 6H, =CMe). ^{13}C-NMR: δ 168.19 (C=N), 148.42, 133.15, 129.44, 118.88 (C_6H_4-4-Me), 20.82 (C_6H_4-4-*Me*), 15.26 (=C*Me*).

(C_6H_4-2-Me)N=C(Me)C(Me)=N(C_6H_4-2-Me) ***(1d)***: ^{1}H-NMR: δ 7.25–6.44 (m, 8H, C_6H_4-2-Me), 2.04 (s, 6H, C_6H_4-2-*Me*) 2.04 (s, 6H, =CMe). ^{13}C-NMR: δ 167.63 (C=N), 147.71, 129.04, 125.88, 125.43, 123.02, 117.18 (C_6H_4-2-Me), 17.71 (C_6H_4-2-*Me*), 15.48 (=C*Me*).

(C_6H_4-4-OMe)N=C(Me)C(Me)=N(C_6H_4-4-OMe) ***(1e)***: ^{1}H-NMR: δ 6.91 (d, 4H, $^3J_{H-H} = 9.4$ Hz, C_6H_4-4-OMe), 6.74 (d, 4H, $^3J_{H-H} = 9.4$ Hz, C_6H_4-4-OMe), 3.80 (s, 6H, C_6H_4-4-O*Me*), 2.16 (s, 6H, =C*Me*). ^{13}C-NMR: δ 168.47 (C=N), 156.42, 144.14, 120.59, 114.30 (C_6H_4-4-OMe), 55.51 (C_6H_4-4-O*Me*), 15.43 (=C*Me*).

(1-$C_{10}H_7$)N=C(Me)C(Me)=N(1-$C_{10}H_7$) ***(1f)***: ^{1}H-NMR: δ 7.85–6.70 (m, 14H, $C_{10}H_7$), 2.23 (s, 6H, =CMe). ^{13}C-NMR: δ 168.88 (C=N), 146.92, 134.02, 127.89, 127.18, 126.11, 125.61, 123.97, 123.25, 112.77 ($C_{10}H_7$), 15.82 (=C*Me*).

(Ph)N=C(Ph)C(Ph)=N(Ph) ***(1g)***: ^{1}H-NMR: δ 7.88–6.44 (m; Ph). ^{13}C-NMR: δ 163.8 (C=N), 149.3, 137.6, 131.0, 128.7, 128.3, 124.8, 120.1 (Ph).

(C_6H_4-4-Me)N = C(Ph)C(Ph) = N(C_6H_4-4-Me) ***(1h)***: ^{1}H-NMR: δ 7.92–6.44 (m, 18H, Ph, C_6H_4-4-Me), 2.24 (s, 6H, C_6H_4-4-*Me*). ^{13}C-NMR: δ 163.7 (C=N), 146.7, 137.6, 134.5, 130.8, 128.9, 128.6, 128.1, 120.3 (Ph, C_6H_4-4-Me), 20.9 (C_6H_4-4-*Me*).

4.4. Preparation of complexes

4.4.1. CpTi[N(C_6H_4-4-OMe)CH=CHN-(C_6H_4-4-OMe)]Cl (**2**)

Magnesium turnings (0.92 g, 38.0 mmol) were added to a solution of $CpTiCl_3$ (8.33 g, 38.0 mmol) and **1a** (10.20 g, 38.0 mmol) in THF (200 ml) at room temperature. After the mixture was stirred for 24 h, the solvent was removed under reduced pressure. The resultant solid was extracted with diethyl ether (200 ml) to give a dark red solution and a white precipitate of magnesium chloride. Concentration and cooling of the filtrate produced **2** as a dark red crystalline solid (9.82 g, 62% yield), m.p. (dec.) 196°C. ^{1}H-NMR (300 MHz, CH_2Cl_2-d_2, 20°C): δ 6.99 (d, 4H, $^3J_{H-H} = 9.2$ Hz, C_6H_4-4-OMe), 6.88 (d, 4H, $^3J_{H-H} = 9.2$ Hz, C_6H_4-4-OMe), 6.52 (s, 5H, Cp), 6.42 (s, 2H, HC=CH), 3.80 (s, 6H, C_6H_4-4-O*Me*). ^{13}C-NMR (75 Mz, CH_2Cl_2-d_2, 25°C): δ 157.2 (*i*-C_6H_4-4-OMe), 146.8 (*p*-C_6H_4-4-OMe), 123.1, 119.5 (*o*,*m*-C_6H_4-4-OMe), 113.8 (Cp), 107.1 (HC=CH), 55.8 (C_6H_4-4-O*Me*). IR (Nujol): ν 1582 (s), 1576 (m), 1478 (m), 1452 (s), 1444 (m), 1440 (m), 1304 (m), 1246 (s), 1204 (w), 1182 (w), 1114 (w), 1082 (w), 1016 (w), 964 (m), 900 (w), 816 (m), 796 (m), 784 (w), 764 (w), 725 (w), 704 (s), 692 (w). EIMS (m/z, %): 416 (100) [M^+], 351 (5) [$M^+ - Cp$], 267 (87) [$C_{16}H_{16}N_2O_2^+$], 134 (19) [$C_8H_8NO^+$]. Anal. Found: C, 59.89; H, 5.04; N, 6.82. Calc. for $C_{21}H_{21}N_2O_2ClTi$ (416.74 g mol^{-1}): C, 60.52; H, 5.08; N, 6.72%.

4.4.2. CpTi[N(C_6H_4-2-Me)C(Me)=C(Me)N(C_6H_4-2-Me)]Cl (*rac*-**3**/*meso*-**3**)

A solution of $CpTiCl_3$ (9.00 g, 41.0 mmol) and 10.84 g (41.0 mmol) **1d** in THF (250 ml) was treated with magnesium turnings (1.00 g, 41.0 mmol) at room temperature. The reaction was carried out as outlined for **2** to give dark red crystals of **3** as a mixture of *rac*-**3** and *meso*-**3** (ratio *rac*-**3**/*meso*-**3** ca. 1:2, determined by ^{1}H-NMR) in 81% yield (13.71 g, m.p. (dec.) 138°C). ^{1}H-NMR (300 MHz, THF-d_8, 20°C): *meso*-**3** δ 7.30–6.90 (m, C_6H_4-2-Me), 6.18 (s, Cp), 1.91 (s, MeC=CMe), 1.87 (s, C_6H_4-2-*Me*). *rac*-**3** δ 7.30–6.90 (m, C_6H_4-2-Me), 6.11 (s, Cp), 2.31, 1.96, 1.88, 1.84 (s, MeC=CMe, C_6H_4-2-*Me*). ^{13}C-NMR (75 MHz, THF-d_8, 25°C): *meso*-**3** δ 151.70 (*i*-C_6H_4-2-Me), 131.73 (*o*-C_6H_4-2-Me), 130.86, 128.15, 127.20, 126.46 (C_6H_4-2-Me), 113.37 (Cp), 113.02 (Me*C*=*C*Me), 18.22 (C_6H_4-2-*Me*), 14.44 (*Me*C=C*Me*). *rac*-**3** δ 152.78, 151.91 (*i*-C_6H_4-2-Me), 131.07, 127.63, 127.15, 126.95, 126.26, 124.70 (C_6H_4-2-Me), 115.16, 114.48 (Me*C*=*C*Me), 113.02 (Cp), 19.00, 17.73 (C_6H_4-2-*Me*), 14.27, 14.21 (*Me*C=C*Me*). EIMS (*m*/*z*, %): 412 (85) [M^+], 376 (10) [$M^+ - Cl$], 249 (11) [$C_{17}H_{17}N_2^+$], 132 (69) [$C_9H_{10}N^+$]. Anal. Found: C, 66.40; H, 6.21; N 6.70. Calc. for $C_{23}H_{25}N_2ClTi$ (412.80 g mol^{-1}): C, 66.92; H, 6.10; N, 6.79%.

4.4.3. CpTi[N(C_6H_4-4-Me)C(Ph)=C(Ph)N(C_6H_4-4-Me)]Cl (**5**)

A solution of $CpTiCl_3$ (5.92 g, 27.0 mmol) and 10.49 g (27.0 mmol) **1h** in THF (250 ml) was treated with magnesium turnings (0.66 g, 27.0 mmol) at room temperature. The reaction was carried out as outlined for **2** to give dark red crystals of **5** (10.87 g, 75% yield, m.p. (dec.) 165°C). ^{1}H-NMR (300 MHz, CH_2Cl_2-d_2, 20°C): δ 7.65 (m, 4H), 7.22 (m, 10H), 6.95 (d, 4H, Ph, C_6H_4-4-Me), 6.39 (s, 5H, Cp), 2.23 (s, 6H, C_6H_4-4-*Me*). ^{13}C-NMR (75 MHz, CH_2Cl_2-d_2, 25°C): δ 150.2, 136.2, 134.7, 132,2, 129.2, 127.5, 127.4, 124.1 (Ph, C_6H_4-4-Me), 119.5 (Ph*C*=*C*Ph), 114.6 (Cp), 20.9 (C_6H_4-4-*Me*). IR (Nujol): ν 1581 (s), 1573 (s), 1564 (s), 1482 (m), 1448 (m), 1424 (m), 1419 (m), 1384 (m), 1380 (m), 1376 (m), 1340 (m), 1324 (m), 1312 (m), 1282 (m), 1034 (m), 984 (m), 812 (m), 792 (m), 764 (m), 698 (m). EIMS (*m*/*z*, %): 536 (35) [M^+], 388 (70) [$C_{28}H_{24}N_2^+$], 194 (100) [$C_{14}H_{12}N^+$], 148 (9) [$C_5H_5ClTi^+$]. Anal. Found: C, 73.14; H, 5.52; N, 5.48. Calc. for $C_{33}H_{29}N_2ClTi$ (536.92 g mol^{-1}): C, 73.82; H, 5.44; N, 5.22%.

4.4.4. CpZr[N(C_6H_4-4-OMe)CH=CHN(C_6H_4-4-OMe)]Cl (**6**)

An amount of 3.05 g (11.6 mmol) of $CpZrCl_3$ was dissolved in THF (150 ml) at -20°C, and **1a** (3.11 g, 11.6 mmol) and magnesium turnings (0.282 g, 11.6 mmol) were added to the solution at this temperature. The solution was allowed to warm to room temperature and stirred for another 24 h. The solvent was then removed in vacuo, and the residue was extracted with diethyl ether (200 ml) and filtered. After the filtrate was concentrated, crystallization was carried out at 0°C to give 4.22 g (79%) **6** as yellow crystals (m.p. (dec.) 225–230°C). ^{1}H-NMR (300 MHz, THF-d_8, 20°C): δ 7.00 (d, 4H, $^3J_{H-H} = 9.0$ Hz, C_6H_4-4-OMe), 6.83 (d, 4H, $^3J_{H-H} = 8.9$ Hz, C_6H_4-4-OMe), 6.52 (s, 5H, Cp), 5.98 (s, 2H, HC=CH), 3.74 (s, 6H, C_6H_4-4-O*Me*). ^{13}C-NMR (75 MHz, THF-d_8, 25°C): δ 156.16 (*p*-C_6H_4-4-OMe), 146.35 (*i*-C_6H_4-4-OMe), 121.93, 114.78 (C_6H_4-4-OMe), 112.05 (Cp), 109.94 (HC=CH), 55.58 (C_6H_4-4-O*Me*). EIMS (*m*/*z*, %): 459 (100) [M^+], 443 (22) [$M^+ - CH_3$], 428 (25) [$M^+ - 2CH_3$], 268 (12) [$C_{16}H_{16}N_2O_2^+$], 134 (11) [$C_8H_8NO^+$]. Anal. Found: C, 53. 90; H, 4.52; N, 6.18. Calc. for $C_{21}H_{21}N_2O_2ClZr$ (460.09 g mol^{-1}): C, 54.82; H, 4.60; N, 6.09%.

4.4.5. CpZr[N(C_6H_4-4-OMe)C(Me)=C(Me)N(C_6H_4-4-OMe)]Cl (**7**)

Magnesium turnings (0.18 g, 7.4 mmol) were added to a solution of $CpZrCl_3$ (1.94 g, 7.4 mmol) and **1e** (2.19 g, 7.4 mmol) in THF (100 ml) at room temperature. The reaction procedure and workup of the reaction was the same as described for the synthesis of **6**. Recrystallization from CH_2Cl_2 gave **7** as yellow crystals in 54% yield (1.79 g, m.p. (dec.) 174–178°C). ^{1}H-NMR (300 MHz, THF-d_8, 20°C): δ 6.65 (s, 8H, C_6H_4-4-OMe), 6.10 (s, 5H, Cp), 3.55 (s, 6H, C_6H_4-4-O*Me*), 1.96 (s, 6H, MeC=CMe). ^{13}C-NMR (75 MHz, THF-d_8, 25°C): δ 156.6 (s, *p*-C_6H_4-4-OMe), 145.9 (s, *i*-C_6H_4-4-OMe), 124.3 (d, $^1J_{C-H} = 158.0$ Hz, C_6H_4-4-OMe), 115.1 (d, $^1J_{C-H} = 156.5$ Hz, C_6H_4-4-OMe), 121.5, (s, Me*C*=*C*Me), 112.1 (d, $^1J_{C-H} = 173.7$ Hz, Cp), 56.1 (q, $^1J_{C-H} = 142.9$ Hz, C_6H_4-4-O*Me*), 15.9 (q, $^1J_{C-H} = 127.8$ Hz, *Me*C=C*Me*). IR (Nujol): ν 3036 (m), 2956 (m), 2948 (s), 2924 (s), 1618 (m), 1604 (s), 1586 (m), 1578 (m), 1482 (s), 1468 (m), 1356 (w), 1326 (sh), 1290 (m), 1204 (w), 1192 (w), 1184 (w), 1168 (w), 1110 (m), 1068 (m), 900 (w). Anal. Found: C, 54.81; H, 5.11; N, 5.89. Calc. for $C_{23}H_{25}N_2O_2ClZr$ (488.14 g mol^{-1}): C, 56.59; H, 5.16; N, 5.74%.

4.4.6. CpZr[N(C_6H_4-4-Me)C(Ph)=C(Ph)N(C_6H_4-4-Me)]Cl (**8**)

Activated magnesium turnings (0.238 g, 9.8 mmol) were added to a solution of $CpZrCl_3$ (2.57 g, 9.8 mmol) and **1h** (3.81 g, 9.8 mmol) in THF (150 ml) at room temperature. The reaction procedure and workup of the reaction was the same as described for the synthesis of **6**. Recrystallization from CH_2Cl_2 gave **8** as ocher crystals in 51% yield (4.04 g, m.p. (dec.) 185°C). ^{1}H-NMR (300 MHz, THF-d_8, 20°C):δ 7.15–6.77 (m, 18H, Ph, C_6H_4-4-Me), 6.22 (s, 5H, Cp), 2.06 (s, 6H, C_6H_4-4-*Me*).

^{13}C-NMR (75 MHz, THF-d_8, 25°C): δ 151.5 (*i*-C_6H_4-4-Me), 139.9 (*p*-C_6H_4-4-Me), 131.3 (*i*-Ph), 133.1, 130.3, 128.4, 127.8, 122.9 (Ph, C_6H_4-4-Me), 116.6 (Ph*C*=*C*Ph), 113.9 (Cp), 21.4 (C_6H_4-4-*Me*). EIMS (*m*/*z*, %): 579 (100) [M^+], 388 (70) [$C_{28}H_{24}N_2^+$], 194 (92) [$C_{14}H_{12}N^+$], 105 (7) [$C_7H_7N^+$], 91 (18) [$C_7H_7^+$]. Anal. Found: C, 66.79; H, 5.14; N, 5.06. Calc. for $C_{33}H_{29}N_2ClZr$ (580.28 g mol^{-1}): C, 68.31; H, 5.04; N, 4.83%.

4.4.7. CpTi[N(C_6H_4-4-OMe)C(Me)=C(Me)N(C_6H_4-4-OMe)]CH_2Ph (9)

Benzylmagnesium chloride (5.00 ml, 3.30 mmol, 0.66 M in diethyl ether) was added dropwise to a solution of **4** (1.47 g, 3.30 mmol) in diethyl ether (100 ml) at −60°C. After the reaction mixture was warmed to room temperature stirring was continued for 8 h. The solvent was then removed in vacuo, and the residue was extracted with pentane (75 ml) to give a red solution and a precipitate of magnesium chloride. Concentration and cooling of the filtrate produced **9** as a red crystalline solid (1.12 g, 68% yield). ^{1}H-NMR (300 MHz, THF-d_8, *20°C*): δ 6.96–6.56 (m, 5H, $CH_2C_6H_5$), 6.74 (s, 8H, C_6H_4-4-OMe), 5.85 (s, 5H, Cp), 3.67 (s, 6H, C_6H_4-4-O*Me*), 2.07 (s, 6H, MeC=CMe), 1.02 (s, 2H, $CH_2C_6H_5$). ^{13}C-NMR (75 MHz, THF-d_8, 25°C): δ 157.4, 146.5, 124.4, 114.5 (C_6H_4-4-OMe), 151.7, 128.4, 126.5, 120.7 ($CH_2C_6H_5$), 114.6 (Me*C*=*C*Me), 113.2 (Cp), 57.3 (t, $^1J_{C-H}$=122.0 Hz, $CH_2C_6H_5$), 55.6 (C_6H_4-4-O*Me*), 15.4 (*Me*C=C*Me*). EIMS (*m*/*z*, %): 500 (18) [M^+], 409 (75) [$M^+ - CH_2C_6H_5$], 148 (100) [$MeOC_6H_4NCMe^+$]. Anal. Found: C, 71.52; H, 6.38; N; 9.72. Calc. for $C_{30}H_{32}N_2O_2Ti$ (500.48 g mol^{-1}): C, 72.00; H, 6.44; N, 9.57%.

4.4.8. CpZr[N(C_6H_4-4-OMe)C(Me)=C(Me)N(C_6H_4-4-OMe)]CH_2Ph (10)

A diethyl ether solution of benzylmagnesium chloride (5.00 ml, 3.30 mmol, 0.66 M) was added dropwise to a slurry of **7** (1.61 g, 3.30 mmol) in diethyl ether (50 ml) at −60°C. Upon warming to room temperature, a homogeneous yellow solution was formed. This solution was stirred for 12 h, and the solvent was removed in vacuo. The residue was treated with pentane (100 ml). After magnesium chloride was removed by filtration, the pentane solution was concentrated to ca. 50 ml. From this concentrated solution, yellow **10** crystallized at 0°C (1.08 g, 60% yield, m.p. (dec.) 154–158°C). ^{1}H-NMR (300 MHz, THF-d_8, *20°C*): δ 7.20–6.55 (m, 13H, $CH_2C_6H_5$, C_6H_4-4-OMe), 6.27 (s, 5H, Cp), 3.72 (s, 6H, C_6H_4-4-O*Me*), 1.91 (s, 6H, MeC=CMe), 1.73 (s, 2H, $CH_2C_6H_5$). EIMS (*m*/*z*, %): 513 (2) [$M^+ - OMe$], 347 (53) [$C_{18}H_{12}N_2Zr^+$], 296 (49) [$C_{18}H_{20}N_2O_2^+$], 148 (100) [$C_9H_{10}NO^+$], 91 (10) [$C_7H_7^+$]. Anal. Found: C, 65.82; H, 5.46; N, 5.27. Calc. for $C_{30}H_{32}N_2O_2Zr$ (543.82 g mol^{-1}): C, 66.25; H, 5.93; N, 5.15%.

4.4.9. CpZr[N(C_6H_4-4-Me)C(Ph)=C(Ph)N(C_6H_4-4-Me)]CH_3 (11)

To a cooled (−40°C) solution of 1.16 g (2.80 mmol) of **8** in diethyl ether (100 ml) were added 2.80 ml of an 1.0 M etheral methylmagnesium iodid (2.80 mmol) solution. On warming to room temperature the solution was stirred for another 6 h. The solvent was then removed in vacuo, and the pale yellow residue was extracted with diethyl ether (150 ml). Concentration and cooling of the filtrate produced **11** as a yellow crystalline solid in 61% yield (0.96 g, m.p. (dec.) 132–134°C). ^{1}H-NMR (300 MHz, THF-d_8, 20°C): δ 7.30–7.00 (m, 18H, Ph, C_6H_4-4-Me), 6.52 (s, 5H, Cp), 2.35 (s, 6H, C_6H_4-4-*Me*), −0.20 (s, 3H, ZrMe). ^{13}C-NMR (75 MHz, THF-d_8, 25°C): δ 152.2 (s, *i*-C_6H_4-4-Me), 140.7 (s, *p*-C_6H_4-4-Me), 132.6 (d, $^1J_{C-H}$ = 159.4 Hz), 130.1 (d, $^1J_{C-H}$ = 155.1 Hz, Ph, C_6H_4-4-Me), 129.5 (s, *i*-Ph), 128.4 (d, $^1J_{C-H}$ = 157.5 Hz), 127.5 (d, $^1J_{C-H}$ = 159.4 Hz, Ph, C_6H_4-4-Me), 125.9 (s, Ph*C*=*C*Ph), 121.6 (d, $^1J_{C-H}$ = 156.6 Hz, Ph, C_6H_4-4-Me), 112.9 (d, $^1J_{C-H}$ = 172.3 Hz, Cp), 21.3 (q, $^1J_{C-H}$ = 125.0 Hz, C_6H_4-4-*Me*), 20.7 (q, $^1J_{C-H}$ = 113.0 Hz, ZrMe). IR (Nujol): *v* 2952 (m), 2924 (s), 2856 (m), 1616 (m), 1586 (m), 1576 (m), 1486 (m), 1458 (s), 1376 (m), 1292 (m), 1220 (m), 1180 (m), 1140 (w), 1048 (w), 988 (w). EIMS (*m*/*z*, %): 558 (43) [M^+], 543 (47) [$M^+ - Me$], 288 (100) [$C_{28}H_{24}N_2^+$], 194 (75) [$C_{19}H_{12}N^+$]. Anal. Found: C, 71.58; H, 5.38; N, 5.42. Calc. for $C_{34}H_{32}N_2Zr$ (559.86 g mol^{-1}): C, 72.94; H, 5.76; N, 5.00%.

4.4.10. CpZr[N(C_6H_4-4-OMe)CH=CHN(C_6H_4-4-OMe)][N(C_6H_4-4-Me)=C(Me)CH=C(Me)O] (12)

A solution of 1.02 g (5.4 mmol) of sodium(acetylacetone-*p*-tolyliminate) (generated by treatment of *p*-tolyliminoacetylacetone (C_6H_4 - 4 - Me)N=C(Me)CH=C(Me)OH (1.02 g, 5.4 mmol) with sodium (0.126 g, 5.5 mmol) in THF (50 ml)) was added dropwise at 0°C to a suspension of **7** (2.48 g, 5.4 mmol) in THF (50 ml). The reaction mixture was warmed to room temperature. After stirring for another 3 h the solvent was removed in vacuo and the residue was extracted with diethyl ether (100 ml). The extract was concentrated to 25 ml and cooled to −20°C to give the product **12** as yellow crystals (2.75 g, 83% yield, m.p. 116–117°C). ^{1}H-NMR (300 MHz, THF-d_8, *20°C*): δ 7.16 (d, 1H, $^3J_{H-H}$ = 8.0 Hz, C_6H_4-4-Me), 7.03 (d, 1H, $^3J_{H-H}$ = 8.8 Hz, C_6H_4-4-OMe), 6.92 (dd, 1H, $^3J_{H-H}$ = 7.8 Hz, $^4J_{H-H}$ = 1.9 Hz, C_6H_4-4-Me), 6.82 (d, 1H, $^3J_{H-H}$ = 8.8 Hz, C_6H_4-4-OMe), 6.54 (d, 1H, $^3J_{H-H}$ = 8.8 Hz, C_6H_4-4-OMe), 6.47 (d, 1H, $^3J_{H-H}$ = 8.4 Hz, C_6H_4-4-Me), 6.37 (s, 5H, Cp), 6.30 (d, 1H, $^3J_{H-H}$ = 8.8 Hz, C_6H_4-4-OMe), 6.12 (dd, 1H, $^3J_{H-H}$ = 8.0 Hz, $^4J_{H-H}$ = 1.9 Hz, C_6H_4-4-Me), 5.92 (d, 1H, $^3J_{H-H}$ = 3.4 Hz, HC=CH), 5.62 (d, 1H, $^3J_{H-H}$ = 3.3 Hz, HC=CH), 5.05 (s, 1H, =C*H*C-

(Me)N), 3.72 (s, 3H, C_6H_4-4-O*Me*), 3.68 (s, 3H, C_6H_4-4-O*Me*), 2.19 (s, 3H, C_6H_4-4-*Me*), 1.69 (s, 3H, OC(Me)=), 1.48 (s, 3H, N=C(*Me*)CH). ^{13}C-NMR (75 MHz, THF-d_8, 25°C): δ 180.22 (N=*C*(Me)CH), 173.88 (O*C*(Me)=), 155.53, 154.86 (*p*-C_6H_4-4-OMe), 148.52, 147.40, 145.56 (*i*-C_6H_4-4-OMe, *i*-C_6H_4-4-Me), 134.75 (*p*-C_6H_4-4-Me), 130.74, 129.66, 125.98, 124.08 (*o*,*m*-C_6H_4-4-Me), 122.38, 119.97, 114.64, 114.16 (*o*,*m*-C_6H_4-4-OMe), 115.42 (N=C(Me)*C*H), 112.24 (Cp), 104.68, 101.23 (HC=CH), 55.58, 55.55 (C_6H_4-4-O*Me*), 25.20, 24.27, 20.93 (C_6H_4-4-*Me*, N=C(*Me*)CH=C(*Me*)O). IR (Nujol): *v* 2934 (s), 2918 (s), 2860 (w), 1608 (m), 1574 (m), 1502 (m), 1458 (m), 1378 (m), 1312 (m), 1274 (m), 1250 (m), 1182 (w), 1166 (w), 1110 (w), 1026 (m), 922 (w), 826 (m), 808 (m), 750 (w). EIMS (*m*/*z*, %): 611 (69) [M^+], 546 (100) [$M^+ - Cp$], 268 (10) [$C_{16}H_{16}N_2O_2^+$], 189 (9) [$C_{12}H_{14}NO^+$], 134 (19) [$C_8H_8NO^+$]. Anal. Found: C, 63.01; H, 5.63; N, 7.14. Calc. for $C_{33}H_{35}N_2O_3Zr$ (612.88 g mol^{-1}): C, 64.67; H, 5.76; N, 6.86%.

4.4.11. [CpTi{N(C_6H_4-2-Me)C(Me)=C(Me)N(C_6H_4-2-Me)}]$_2$O (**13**)

To a solution of **3** (1.20 g, 2.9 mmol, *rac*/*meso*-ratio 1:2) and imidazol $C_3H_4N_2$ (0.40 g, 5.8 mmol) in THF (50 ml) was added via syringe H_2O (27 μl, 1.5 mmol) at room temperature. The reaction mixture was vigorously stirred for 12 h at room temperature, and the solvent was removed under vacuum. The residue was washed with pentane (50 ml), dried under vacuum, and extracted with diethyl ether (100 ml). The extract was concentrated to 50 ml and cooled to −20°C to give the product **13** as red crystals (1.79 g, 80% yield, m.p. 192–194°C). ^{1}H-NMR (300 MHz, THF-d_8, 20°C): *meso*/*meso*-**13**: δ 7.27–6.95 (m, 16H, C_6H_4-2-Me), 5.96 (s, 10H, Cp), 1.92 (s, 12H, C_6H_4-2-*Me*), 1,91 (s, 12H, MeC=CMe). ^{13}C-NMR (75 MHz, THF-d_8, 25°C): δ 152.04 (*i*-C_6H_4-2-Me), 131.66, 130.91, 127.63, 126.76, 124.83 (C_6H_4-2-Me), 112.06 (Me*C*=*C*Me), 111.16 (Cp), 18.38 (*Me*C=C*Me*), 15.28 (C_6H_4-2-*Me*). IR (Nujol): *v* 2964 (m), 2872 (m), 1592 (m), 1460 (s), 1376 (m), 1326 (m), 1250 (m), 1116 (w), 1016 (w), 978 (w), 800 (s), 740 (m), 610 (w), 434 (m). EIMS (*m*/*z*, %): 770 (100) [M^+], 506 (50) [$M^+ - DAD$], 376 (18) [$C_{23}H_{25}N_2Ti^+$], 346 (40) [$C_{21}H_{19}N_2Ti^+$], 264 (20) [$C_{18}H_{20}N_2^+$]. Anal. Found: C, 70.98; H, 6.36; N, 7.65. Calc. for $C_{46}H_{50}N_4OTi_2$ (770.69 g mol^{-1}): C, 71.69; H, 6.54; N, 7.27%.

4.4.12. Cp$_2$Ti[N(C_6H_4-4-Me)C(Me)=C(Me)N(C_6H_4-4-Me)] (**15**)

Magnesium turnings (0.244 g, 10.04 mmol) were added to a solution of Cp_2TiCl_2 (2.50 g, 10.04 mmol) and **1c** (2.65 g, 10.04 mmol) in THF (100 ml) at room temperature. After the mixture was stirred for 12 h, the solvent was removed under reduced pressure. The resultant solid was dissolved in pentane (100 ml), the solution was filtered and concentrated (50 ml), and dark green crystals of **15** were obtained by crystallization at 0°C (3.46 g, 78% yield, m.p. (dec.) 140–142°C). ^{1}H-NMR (300 MHz, CH_2Cl_2-d_2, −50°C): δ 7.20–6.40 (m, 8H, C_6H_4-4-Me), 5.50 (s, 5H, Cp), 5.45 (s, 5H, Cp), 2.33 (s, 6H, C_6H_4-4-*Me*), 1.94 (s, 6H, =CMe). 25°C: δ 7.18–6.40 (m, 8H, C_6H_4-4-Me), 5.50 (s, 10H, Cp), 2.35 (s, 6H, C_6H_4-4-*Me*), 2.00 (s, 6H, =CMe). ^{13}C-NMR (75 MHz, CH_2Cl_2-d_2, −50°C): δ 150.29 (*i*-C_6H_4-4-Me), 128.47, 128.32 (*m*-C_6H_4-4-Me), 127.91 (*p*-C_6H_4-4-Me), 123.92, 122.89 (*o*-C_6H_4-4-Me), 131.42 (C=C), 108.37, 102.34 (Cp), 20.75 (C_6H_4-4-*Me*), 17.14 (=C*Me*). 25°C: δ 151.08 (*i*-C_6H_4-4-Me), 128.53 (*o*-C_6H_4-4-Me), 128.40 (*p*-C_6H_4-4-Me), 123.64 (br, *m*-C_6H_4-4-Me), 108.69, 102.58 (br, Cp), 131.67 (C=C), 20.70 (C_6H_4-4-*Me*), 17.05 (=C*Me*). IR (KBr): *v*=3017 (w), 2918 (w), 1605 (m), 1500 (vs), 1441 (m), 1354 (vs), 1317 (s), 1301 (m), 1258 (vs), 1106 (m), 1017 (m), 809 (s), 803 (s), 781 (vs). EIMS (*m*/*z*, %): 442 (73) [M^+], 377 (31) [$M^+ - Cp$], 178 (100) [$C_{10}H_{10}Ti^+$]. Anal. Found: C, 75.78; H, 6.70; N, 6.31. Calc. for $C_{28}H_{30}N_2Ti$ (442.44 g mol^{-1}): C, 76.01; H, 6.83; N, 6.33%.

4.4.13. Cp$_2$Ti[N(C_6H_4-2-Me)C(Me)=C(Me)N(C_6H_4-2-Me)] (*rac*/*meso*-**16**)

This compound was prepared in a manner analogous to that used for the synthesis of **15**. Activated magnesium turnings (0.328 g, 13.50 mmol) were added to a solution of Cp_2TiCl_2 (3.36 g, 13.50 mmol) and **1d** (3.57 g, 13.50 mmol) in THF (150 ml) at room temperature to give a mixture of *rac*-**16** and *meso*-**16** of about 10:1 as a redbrown crystalline solid in overall 54% yield (3.23 g). ^{1}H-NMR (300 MHz, toluene-d_8, 20°C): *rac*-**16** δ 7.15–6.40 (m, C_6H_4-2-Me), 5.43, 5.30 (s, Cp), 2.19, 1.99 (s, =CMe), 1.63, 1.53 (s, C_6H_4-2-*Me*). *meso*-**16** δ 7.15-6.40 (m, C_6H_4-2-Me), 5.33, 5.26 (s, Cp), 1.98 (s, =CMe), 1.54 (s, C_6H_4-2-*Me*). 90°C: *rac*-**16** δ 7.20–6.38 (m, C_6H_4-2-Me), 5.37 (s, Cp), 2.10 (s, =CMe), 1.61 (s, C_6H_4-2-*Me*). *meso*-**16** δ 7.20–6.38 (m, C_6H_4-2-Me), 5.36, 5.25 (s, Cp), 1.97, 1.59 (s, =CMe). ^{13}C-NMR (75 MHz, CH_2Cl_2-d_2, 25°C): *meso*-**16** δ 152.43 (*i*-C_6H_4-2-Me), 131.05, 127.42, 125.97, 125.68, 123.12 (C_6H_4-2-Me), 130.17 (C=C), 108.57, 102.57 (Cp), 18.29 (C_6H_4-2-*Me*), 16.49 (=C*Me*). IR (KBr): *v* 3012 (w), 2945 (w), 2920 (w), 1594 (s), 1479 (vs), 1457 (s), 1441 (s), 1354 (vs), 1317 (m), 1301 (m), 1249 (vs), 1017 (m), 805 (vs), 741 (vs). EIMS (*m*/*z*, %): 442 (39) [M^+], 377 (57) [$M^+ - Cp$], 178 (100) [$C_{10}H_{10}Ti^+$], 113 (21) [$C_5H_5Ti^+$]. Anal. Found: C, 76.22; H, 6.90; N, 6.25. Calc. for $C_{28}H_{30}N_2Ti$ (442.44 g mol^{-1}): C, 76.01; H, 6.83; N, 6.33%.

4.4.14. Cp$_2$Ti[N(C_6H_4-4-OMe)C(Me)=C(Me)N(C_6H_4-4-OMe)] (**17**)

This compound was prepared in a manner analogous to that used for the synthesis of **15**. Activated magne-

sium turnings (0.244 g, 10.04 mmol) were added to a solution of Cp_2TiCl_2 (2.50 g, 10.04 mmol) and **1e** (2.98 g, 10.04 mmol) in THF (150 ml) at room temperature to give **17** as a dark green crystalline solid (3.14 g, 66% yield, m.p. (dec.) 160°C). ^{1}H-NMR (300 MHz, CH_2Cl_2-d_2, −50°C): δ 6.90–6.23 (m, 8H, C_6H_4-4-OMe), 5.45, 5.40 (s, 5H, Cp), 3.75 (s, 6H, C_6H_4-4-O*Me*), 1.91 (s, 6H, =CMe). 20°C: δ 6.85–6.54 (m, 8H, C_6H_4-4-OMe), 5.47 (s, 10H, Cp), 3.79 (s, 6H, C_6H_4-4-O*Me*), 1.95 (s, 6H, =CMe). ^{13}C-NMR (75 MHz, CH_2Cl_2-d_2, −50°C): δ 154.76 (*i*-C_6H_4-4-OMe), 146.46 (*p*-C_6H_4-4-OMe), 124.58, 123.64 (*m*-C_6H_4-4-OMe), 112.82, 112.48 (*o*-C_6H_4-4-OMe), 128.07 (C=C), 108.24, 102.17 (Cp), 55.27 (C_6H_4-4-O*Me*), 17.05 (=C*Me*). 25°C: δ 155.51 (*i*-C_6H_4-4-Me), 147.28 (*p*-C_6H_4-4-OMe), 124.28 (br, *m*-C_6H_4-4-OMe), 113.81 (*o*-C_6H_4-4-OMe), 128.56 (C=C), 108.64, 102.53 (br, Cp), 55.46 (C_6H_4-4-O*Me*), 16.98 (=C*Me*). IR (KBr): *v* 3045 (w), 2925 (w), 2840 (w), 1498 (vs), 1465 (m), 1440 (s), 1356 (s), 1286 (m), 1238 (vs), 1180 (m), 1036 (s), 1019 (s), 840 (m), 805 (s), 803 (s), 787 (vs). EIMS (*m*/*z*, %): 474 (77) [M^+], 409 (83) [M^+ − Cp], 234 (12), 178 (100) [$C_{10}H_{10}Ti^+$], 113 (8) [$C_5H_5Ti^+$]. Anal. Found: C, 70.72; H, 6.17; N, 5.81. Calc. for $C_{28}H_{30}N_2O_2Ti$ (474.44 g mol^{-1}): C, 70.89; H, 6.37; N, 5.90%.

4.4.15. $Cp_2Ti[N(1\text{-}C_{10}H_7)C(Me)=C(Me)N(1\text{-}C_{10}H_7)]$ (*rac*/*meso*-**18**)

This compound was prepared in a manner analogous to that used for the synthesis of **15**. Magnesium turnings (0.328 g, 13.50 mmol) were added to a solution of Cp_2TiCl_2 (3.36 g, 13.50 mmol) and **1f** (4.54 g, 13.50 mmol) in THF (150 ml) at room temperature to give a mixture of *rac*-**18** and *meso*-**18** of about 8:1 as a redbrown crystalline solid in overall 73% yield (5.07 g). ^{1}H-NMR (300 MHz, toluene-d_8, 20°C): *rac*-**18** δ 8.60–6.50 (m, 1-$C_{10}H_7$), 5.64, 5.22 (s, Cp), 1.68, 1.51 (s, =CMe). *meso*-**18** δ 8.60–6.50 (m, 1-$C_{10}H_7$), 5.44, 5.25 (s, Cp), 1.55 (s, =CMe). *90°C*: *rac*-**18** δ 8.25–6.70 (m, 1-$C_{10}H_7$), 5.44 (s, Cp), 1.65 (s, =CMe). *meso*-**18** δ 8.25–6.70 (m, 1-$C_{10}H_7$), 5.48, 5.26 (s, Cp), 1.60 (s, =CMe). ^{13}C-NMR (75 MHz, CH_2Cl_2-d_2, 25°C): *meso*-**18** δ 150.33, 134.14, 129.62, 128.23, 128.07, 125.70, 125.55, 125.45, 123.49, 121.52 (1-$C_{10}H_7$), 129.51 (C=C), 108.83, 102.77 (Cp), 17.11 (=C*Me*). IR (KBr): *v* 3049 (w), 2912 (w), 1569 (s), 1504 (m), 1457 (m), 1390 (vs), 1342 (s), 1329 (m), 1296 (m), 1268 (s), 1233 (s), 1129 (m), 1017 (s), 804 (vs), 783 (vs), 766 (vs). EIMS (*m*/*z*, %): 514 (72) [M^+], 449 (38) [M^+ − Cp], 178 (100) [$C_{10}H_{10}Ti^+$], 127 (26) [$C_{10}H_7^+$], 113 (12) [$C_5H_5Ti^+$]. Anal. Found: C, 79.11; H, 5.74; N, 5.39. Calc. for $C_{34}H_{30}N_2Ti$ (514.50 g mol^{-1}): C, 79.37; H, 5.88; N, 5.44%.

4.4.16. $Cp_2Hf[N(Ph)C(Ph)=C(Ph)N(Ph)]$ (**21**)

To a solution of **1g** (1.37 g, 3.80 mmol) in THF (100 ml) was added sodium in small pieces (0.175 g, 7.60 mmol), and the mixture was stirred overnight at room temperature until the sodium was completely dissolved. The dark red solution of Na_2[N(Ph)C(Ph)=C(Ph)N(Ph)] was added dropwise at −20°C to a solution of Cp_2HfCl_2 (1.44 g, 3.79 mmol) in THF (100 ml). After stirring for another 6 h at room temperature the solvent was removed in vacuo and the residue was extracted with pentane (150 ml). The extract was concentrated to 75 ml and cooled to −20°C to give **21** as yellow-orange crystals (1.75 g, 69% yield, m.p. (dec.) 153–155°C). ^{1}H-NMR (300 MHz, CH_2Cl_2-d_2, −50°C): δ 7.40–6.50 (m, 20H, C_6H_5), 6.28, 5.77 (s, 5H, Cp). 20°C: δ 7.28–6.79 (m, 20H, C_6H_5), 6.03 (s, 10H, Cp). ^{13}C-NMR (75 MHz, CH_2Cl_2-d_2, 25°C): δ 153.75 (*N*-*i*-C_6H_5), 138.83 (C-*i*-C_6H_5), 129.84 (C=C), 132.12, 128.29, 127.41, 126.68, 125.23, 121.92 (C_6H_5), 108.80 (Cp). IR (KBr): *v* 3062 (w), 3022 (w), 2945 (w), 2913 (w), 1591 (vs), 1484 (vs), 1435 (m), 1304 (s), 1275 (vs), 1073 (m), 1018 (s), 960 (m), 819 (s), 809 (s), 794 (vs), 774 (s), 760 (s), 755 (s), 723 (s), 696 (vs). EIMS (*m*/*z*, %): 670 (100) [M^+], 360 (12) [$C_{26}H_{20}N_2^+$], 180 (29) [$C_{13}H_{10}N^+$], 77 (39) [$C_6H_5^+$]. Anal. Found: C, 64.30; H, 4.55; N, 4.32. Calc. for $C_{36}H_{30}N_2Hf$ (669.14 g mol^{-1}): C, 64.62; H, 4.52; N, 4.19%.

5. Supplementary material

Crystallographic data for the structural analysis have been deposited with the Cambridge Crystallographic Data Center, CCDC nos. 150571, 150568, 150569 and 150570 for compounds **9**, **12**, **13** and **21**, respectively. Copies of this information may be obtained free of charge from The Director, CCDC, 12 Union Road, Cambridge CB2 1EZ, UK (fax: +44-1223-336033; e-mail: deposit@ccdc.cam.ac.uk or www: http://www.ccdc.cam.ac.uk).

Acknowledgements

Prof. Dr D. Steinborn (Martin-Luther-Universität Halle-Wittenberg) is kindly acknowledged for providing laboratory facilities. We thank Dr F. Girgsdies (Technische Universität Berlin) for help with the X-ray diffraction analyses. This work has been financially supported by the Deutsche Forschungsgemeinschaft and Bayer AG.

References

[1] Not included are diamide ligands which act as tridentate ligand system by an additional donor atom. (a) W.A. Herrmann, M. Denk, R.W. Albach, J. Behm, E. Herdtweck, Chem. Ber. 124 (1991) 683. (b) T.H. Warren, R.R. Schrock, W.M. Davis,

Organometallics 15 (1996) 562. (c) K. Aoyagi, P.K. Gantzel, K. Kalai, T.D. Tilley, Organometallics 15 (1996) 923. (d) S. Tinkler, R.J. Deeth, D.J. Duncalf, A. McCamley, J. Chem. Soc. Chem. Commun. (1996) 2623. (e) J.D. Scollard, D.H. McConville, J.J. Vittal, Organometallics 16 (1997) 4415. (f) A.D. Horton, J. de With, Organometallics 16 (1997) 5424. (g) N.A.H. Male, M. Thornton-Pett, M. Bochmann, J. Chem. Soc. Dalton Trans. (1997) 2487. (h) B. Tsuie, D.C. Swenson, R.F. Jordan, J.L. Petersen, Organometallics 16 (1997) 1392. (i) L.T. Armistead, P.S. White, M.R. Gagné, Organometallics 17 (1998) 216. (j) T.H. Warren, R.R. Schrock, W.M. Davis, Organometallics 17 (1998) 308. (k) Y.-M. Jeon, S.J. Park, J. Heo, K. Kim, Organometallics 17 (1998) 3161. (l) C.H. Lee, Y.-H. La, S.J. Park, J.W. Park, Organometallics 17 (1998) 3648. (m) Y.-M. Jeon, J. Heo, W.M. Lee, T. Chang, K. Kim, Organometallics 18 (1999) 4107. (n) C.H. Lee, Y.-H. La, J.W. Park, Organometallics 19 (2000) 344. (o) C. Lorber, B. Donnadieu, R Choukroun, Organometallics 19 (2000) 1963.

[2] (a) P.J. Shapiro, E. Bunel, W.P. Schaefer, J.E. Bercaw, Organometallics 9 (1990) 867. (b) D.D. Devore, F.J. Timmers, D.L. Hasha, R.K. Rosen, T.J. Marks, P.A. Deck, Ch.L. Stern, Organometallics 15 (1996) 3132. (c) P.-J. Sinnema, L. van der Veen, A.L. Spek, N. Feldman, J.H. Teuben, Organometallics 16 (1997) 4245. (d) J. Okuda, Th. Eberle, Th. P. Spaniol, Chem. Ber. 130 (1997) 209. (e) L. Schwink, P. Knochel, T. Eberle, J. Okuda, Organometallics 17 (1998) 7. (f) Th. Eberle, Th. P. Spaniol, J. Okuda, Eur. J. Inorg. Chem. (1998) 237.

[3] (a) J.D. Scollard, D.H. McConville, N.C. Payne, J.J. Vittal, Macromolecules 29 (1996) 5241. (b) J.D. Scollard, D.H. McConville, J. Am. Chem. Soc. 118 (1996) 10008. (c) J.D. Scollard, D.H. McConville, St. J. Rettig, Organometallics 16 (1997) 1810.

[4] V.C. Gibson, B.S. Kimberley, A.J.P. White, D.J. Williams, Ph. Howard, J. Chem. Soc. Chem. Commun. (1998) 313.

[5] (a) St.L. Latesky, A.K. McMullen, G.P. Niccolai, I.P. Rothwell, Organometallics 4 (1985) 1896. (b) F.G.N. Cloke, H.C. de Lemos, A.A. Sameh, J. Chem. Soc. Chem. Commun. (1986) 1344. (c) L.R. Chamberlain, L.D. Durfee, Ph.E. Fanwick, L.M. Kobriger, St.L. Latesky, A.K. McMullen, B.D. Steffey, I.P. Rothwell, K. Folting, J.C. Huffman, J. Am. Chem. Soc. 109 (1987) 6068. (d) B. Hessen, J.E. Bol, J.L. de Boer, A. Meetsma, J.H. Teuben, J. Chem. Soc. Chem. Commun. (1989) 1276. (e) H. tom Dieck, H.J. Rieger, G. Fendesak, Inorg. Chim. Acta 177 (1990) 191. (f) W.A. Herrmann, M. Denk, W. Scherer, F.-R. Klingan, J. Organomet. Chem. 444 (1993) C21. (g) F.J. Berg, J.L. Petersen, Organometallics 12 (1993) 3890. (h) K. Dreisch, C. Andersson, C. Stålhandske, Polyhedron 12 (1993) 303 and 1335. (i) L.G. Hubert-Pfalzgraf, A. Zaki, L. Toupet, Acta Crystallogr. C 49 (1993) 1609. (j) L. Kloppenburg, J.L. Petersen, Organometallics 16 (1997) 3548. (k) R. Leigh Huff, S.-Y.S. Wang, K.A. Abboud, J.M. Boncella, Organometallics 16 (1997) 1779. (l) M.J. Scott, S.J. Lippard, Organometallics 16 (1997) 5857. (m) K. Mashima, Y. Matsuo, K. Tani, Chem. Lett. (1997) 767. (n) T. Zippel, P. Arndt, A. Ohff, A. Spannenberg, R. Kempe, U. Rosenthal, Organometallics 17 (1998) 4429. (o) K. Mashima, Y. Matsuo, K. Tani, Organometallics 18 (1999) 1471. (p) M.G. Thorn, Ph.E. Fanwick, I.P. Rothwell, Organometallics 18 (1999) 4442.

[6] (a) J. Scholz, M. Dlikan, D. Ströhl, A. Dietrich, H. Schumann, K.-H. Thiele, Chem. Ber. 123 (1990) 2279. (b) J. Scholz, A. Dietrich, H. Schumann, K.-H. Thiele, Chem. Ber. 124 (1991) 1035. (c) R. Goddard, C. Krüger, G.A. Hadi, K.-H. Thiele, J. Scholz, Z. Naturforsch. 49b (1994) 519. (d) J. Scholz, B. Richter, R. Goddard, C. Krüger, Chem. Ber. 126 (1993) 57. (e) B. Richter, J. Scholz, B. Neumüller, R. Weimann, H. Schumann, Z. Anorg. Allg. Chem. 621 (1995) 365. (f) H. Görls, B. Neumüller, A. Scholz, J. Scholz, Angew. Chem. 107 (1995) 732; Angew. Chem. Int. Ed. Engl. 34 (1995) 673. (g) J. Wunderle, J. Scholz, U. Baumeister, H. Hartung, Z. Kristallogr. 211 (1996) 423. (h) H. Görls, J. Scholz, J. Organomet. Chem., in press.

[7] B. Richter, J. Scholz, J. Sieler, K.-H. Thiele, Angew. Chem. 107 (1995) 2865; Angew. Chem. Int. Ed. Engl. 34 (1995) 2649.

[8] G.J. Pindado, M. Thornton-Pett, M. Bochmann, J. Chem. Soc. Dalton Trans. (1998) 393.

[9] (a) G.A. Hadi, J. Wunderle, K.-H. Thiele, R. Froehlich, Z. Kristallogr. 209 (1994) 372. (b) G.A. Hadi, J. Wunderle, K.-H. Thiele, H. Langhof, Z. Kristallogr. 209 (1994) 373.

[10] The terms *prone* and *supine* used in this text to describe the mode of 1,4-diaza-1,3-diene orientation in the CpTi(DAD)Cl complexes have been introduced originally by Yasuda and Nakamura to express the stereochemistry of early transition metal diene complexes. They proposed this nomenclature because the classical *endo* and *exo* nomenclature does not adequately characterize this type of conformation. H. Yasuda, A. Nakamura, Angew. Chem. 99 (1987) 745; Angew. Chem., Int. Ed. Engl. 26 (1987) 723.

[11] H. Kawaguchi, Y. Yamamoto, K. Asaoka, K. Tatsumi, Organometallics 17 (1998) 4380.

[12] C. Trompke, PhD Thesis, Universität Hamburg, 1993.

[13] J. Scholz, F. Rehbaum, K.-H. Thiele, R. Goddard, P. Betz, C. Krüger, J. Organomet. Chem. 443 (1993) 93.

[14] H. tom Dieck, W. Kollvitz, I. Kleinwächter, W. Rohde, L. Stamp, Transition Met. Chem. 11 (1986) 361.

[15] A. Galindo, A. Ienco, C. Mealli, New J. Chem. 14 (2000) 73.

[16] (a) R.F. Jordan, R.E. LaPointe, C.S. Bajgur, S.F. Echols, R.D. Willett, J. Am. Chem. Soc. 109 (1987) 4111. (b) R.F. Jordan, R.E. LaPointe, N.C. Beanziger, G.D. Hinch, Organometallics 9 (1990) 1539. (c) D.J. Crowther, S.L. Borkowsky, D. Swenson, T.Y. Meyer, R.F. Jordan, Organometallics 12 (1993) 2897. (d) C. Tedesco, A. Immirzi, A. Proto, Acta Crystallogr. B 54 (1998) 431.

[17] M. Mena, M. A. Pellinghelli, P. Royo, R. Serrano, A. Tiripicchio, J. Chem. Soc. Chem. Commun. (1986) 1118.

[18] (a) M. Rahim, N.J. Taylor, S. Xin, S. Collins, Organometallics, 17 (1998) 1315. (b) L. Kakaliou, W.J. Scanlon IV, B. Qian, S.W. Baek, D.H. Motry, Inorg. Chem. 38 (1999) 5964.

[19] K.-H. Thiele, A. Scholz, J. Scholz, U. Böhme, R. Kempe, J. Sieler, Z. Naturforsch. 48b (1993) 1753.

[20] T.T. Nadasdi, Y. Huang, D.W. Stephan, Inorg. Chem. 32 (1993) 347.

[21] (a) D.M. Curtis, S. Thanedar, W.M. Butler, Organometallics 3 (1984) 1855. (b) J.C. Huffman, K.G. Moloy, J.A. Marsella, K.G. Caulton, J. Am. Chem. Soc. 102 (1980) 3009.

[22] (a) U. Thewalt, D. Schomburg, J. Organomet. Chem., 127 (1977) 169. (b) B. Honold, U. Thewalt, M. Herberhold, H.G. Alt, L.B. Kool, M.D. Rausch, J. Organomet. Chem. 314 (1986) 105. (c) T. Carofiglio, C. Floriani, A. Sgamellotti, M. Rosi, A. Chiesi-Villa, C. Rizzoli, J. Chem. Soc. Dalton Trans. (1992) 1081. (d) M. Björgvinsson, S. Halldorsson, I. Arnason, J. Magull, D. Fenske, J. Organomet. Chem. 544 (1997) 207.

[23] (a) F.G. Riddell, The stereodynamics of five-membered nitrogen-containing rings, in: J.B. Lambert, Y. Takeuchi (Eds.), Cyclic Organonitrogen Stereodynamics, VCH, Weinheim, 1992, p. 159. (b) A. Rauk, L.C. Allen, K. Mislow, Angew. Chem. 82 (1970) 453; Angew. Chem. Int. Ed. Engl. 9 (1970) 400. (c) H. Kessler, Angew. Chem. 82 (1970) 237; Angew. Chem. Int. Ed. Engl. 9 (1970) 219.

[24] Other examples which demonstrate that the activation barrier and coalescence temperature for the degenerate interconversion of the five-membered ZrN_2C_2 ring of zirconocene enediamide complexes mainly depends on the substituents at the nitrogen

atoms have been reported by Petersen et al.: $Cp_2^*Zr[N(Me)C(CH_2SiMe_2CH_2)=CN(Me)]$: $\Delta G^{\#} < 42$ kJ mol^{-1} ($T_c < -110$°C), F. Berg, J.L. Petersen, Tetrahedron 48 (1992) 4749. $Cp_2Zr[NC(Me_3)C(CH_2SiMe_2CH_2)=CN(CMe_3)]$: $\Delta G^{\#} = 81.6(\pm 2)$ kJ mol^{-1} ($T_c = 142$°C). $Cp_2Zr[N(C_6H_3\text{-}2,6\text{-}Me_2)C(CH_2SiMe_2CH_2)=CN(CMe_3)]$: $\Delta G^{\#} > 84$ kJ mol^{-1} ($T_c > 150$°C), F. Berg, J.L. Petersen, Organometallics 10 (1991) 1599.

[25] *$CpTiCl_3$*: R.B. King, Organomet. Synth. 1 (1965) 78; R.D. Gorsich, J. Am. Chem. Soc. 82 (1960) 4211. (b) *$CpZrCl_3$*: G. Erker, K. Berg, L. Treschanke, K. Engel, Inorg. Chem. 21 (1982) 1277. (c) *Cp_2TiCl_2*: J.M. Birmingham, Adv. Organomet. Chem. 2 (1964) 365. (d) *Cp_2HfCl_2*: P.M. Druce, B.M. Kingston, M.F. Lappert, I.R. Spalding, R.C. Srivastava, J. Chem. Soc. A (1969) 2106.

[26] M. Siegfried, Ber. Dtsch. Chem. Ges. 25 (1892) 1600. (b) H. von Pechmann, Ber. Dtsch. Chem. Ges. 21 (1888) 1411. (c) J.M. Kliegmann, R.K. Barnes, Tetrahedron 26 (1970) 2555. (d) H. tom Dieck, M. Svoboda, Th. Greiser, Z. Naturforsch. 36b (1980) 823.

[27] MOLEN, An Interactive Structure Solution Procedure, Enraf-Nonius, Delft, The Netherlands, 1990.

[28] Software package STOE.

[29] G.M. Sheldrick, Acta Crystallogr. A 46 (1990) 467.

[30] G.M. Sheldrick, SHELXL-97, University of Göttingen, Germany, 1997.